



ARTICLE

Pathways Related to ROS Production, Clearance, and Signal Transduction during Cold Response in *Brassica napus* L. with Strong Cold Resistance

Weiliang Qi^{1,2,3,4,*}, Wancang Sun⁵, Li Ma⁵, Xiaolong Li¹, Haiqing Liu¹, Cairong Yang⁶ and Ziyao Wei¹

¹School of Agriculture and Bioengineering, Longdong University, Qingyang, 745000, China

²Collaborative Innovation Center for Longdong Dryland Crop Germplasm Improvement and Industrialization, Longdong University, Qingyang, 745000, China

³Gansu Dryland Research Center of Winter Wheat Germplasm Innovation and Application Engineering, Longdong University, Qingyang, 745000, China

⁴Gansu Collaborative Innovation of Academicians and Experts on Dryland Agriculture in the Loess Plateau, Longdong University, Qingyang, 745000, China

⁵Agronomy College, Gansu Agriculture University, Lanzhou, 730070, China

⁶College of Chemistry and Life Sciences, Chengdu Normal University, Chengdu, 611130, China

*Corresponding Author: Weiliang Qi. Email: qwl9196@163.com

Received: 07 November 2024; Accepted: 18 February 2025; Published: 31 March 2025

ABSTRACT: *Brassica napus* L. (*B. napus*), recognized as a significant cash and oil crop, faces challenges in popularization and application in northern China due to its limited cold resistance. Clarifying the mechanism of cold stress on gene regulation and signal transduction in *B. napus* is crucial. To address these issues, we conducted transcriptome sequencing and gene expression analysis, along with gene ontology (GO) and Kyoto encyclopedia of genes and genomes (KEGG) pathway profiling under natural (25°C) and cold (4°C) conditions in cold tolerant 16VHNTS309 and weak cold-resistant Tianyou 2238 *B. napus* seedlings. Enhanced genomic annotation was achieved through additional sequencing. A total of 6127 and 8531 differentially expressed genes (DEG) were identified in 16VHNTS309 and Tianyou 2238, respectively. The expression patterns of 23 DEGs were validated by quantitative real-time PCR (qRT-PCR), confirming the RNA-Seq results. Under cold stress, 58 pathways in 16VHNTS309 demonstrated significant changes (q-Value < 0.05), compared to 9 pathways in Tianyou 2238 (q-Value < 0.05), highlighting *B. napus*' sophisticated regulatory network which aids in managing growth and development challenges. After 48 h of cold stress treatment, genes associated with reactive oxygen species (ROS) clearance, such as those involved in antioxidant VB₆, sulfur metabolism, peroxisomes, and phagosomes, were notably up-regulated in 16VHNTS309, indicating its robust ROS clearance capability. Significant gene expressions within Ca²⁺, MAPK, and transcription factor pathways related to ROS suggest that varieties with strong cold resistance possess a complex signal regulation mechanism. Comprehensive analyses of stomatal cells, physiological parameters of ROS, ABA, and H₂S, along with transcriptomic data, revealed that optimal ROS levels interact with ABA and H₂S to regulate stomatal closure in *B. napus* 16VHNTS309 under the influence of antioxidant enzymes.

KEYWORDS: *Brassica napus* L.; cold stress; comparative transcriptome; ROS

1 Introduction

Cold stress is one of the primary environmental challenges plants face throughout their life cycle. Cold temperatures negatively impact plant growth and development by causing tissue injury and delaying



growth [1], and they significantly restrict the spatial distribution of plants. To adapt, cold-tolerant plants have evolved complex and effective cold-responsive mechanisms, such as changes in leaf tissue structure, accumulation of compatible osmolytes, and both enzymatic and non-enzymatic antioxidative systems [2]. Concurrently, ROS production occurs under cold stress. Prior research has indicated that ROS accumulation can lead to oxidative damage in plant cells, ultimately resulting in cell death. Further investigations into plant signaling molecules have revealed that plants exhibit specific and highly dynamic signaling responses under abiotic stress, with ROS acting as key signaling molecules. Extensive studies have demonstrated the rapid release of ROS under cold stress and their ability to transmit signals over long distances [3,4]. ROS is critical not only for local immune responses but also for cell-to-cell communication. It has been established that ROS interact with other signaling molecules, such as Ca^{2+} [5], MAPK [6], transcription factors [7] (WRKY, etc.), and ABA [8] among others. These interactions are linked to the differential expression of numerous genes [9]. Cold-responsive genes continue to be identified and annotated through transcriptomic methods across various plant species. For example, significant numbers of genes have been identified as cold-responsive in economically important plants like *Arabidopsis* [10], *Camellia sinensis* [11], *Poncirus trifoliata* [12], *Eucalyptus dunnii* [13] and *Beta vulgaris* [14]. Although many cold-regulated genes have been discovered and assigned specific functions across different species, the mechanisms of their cold responses have not been fully elucidated. In addition, genes may be involved in different pathways across species, and various species may have distinct cold-response genes. Therefore, there is a need for further exploration of cold response regulatory pathways and genes across different plants.

Winter rape, an important economic cover crop, offers economic, environmental, and ecological benefits and aids in reducing dust sources in northern China [15]. However, *B. napus* is primarily distributed in regions such as the Loess Plateau, the middle and lower reaches of the Yangtze River, the Huang-Huai Plain, the Yunnan-Guizhou Plateau, Sichuan Basin, and the coastal areas of south China [16]. The growth and development of *B. napus* can be hindered by its poor cold resistance [15]. Previous studies have shown that distant hybridization is a highly effective method for promoting gene or chromosomal segment exchanges and enriching germplasm resources, thus breeding new *B. napus* varieties with biotic or abiotic stress resistance [17]. Zhao et al. [18] and Wang et al. [19] have successfully bred new lines of *B. napus* with high affinity, good yield, disease, or cold resistance through interspecific hybridization, backcross, and continuous self-cross of *B. napus* and *B. rape*. In an effort to overcome the key technical challenges of winter rape overwintering, our research group has developed the cold-resistant *B. napus* variety 16VHNTS309, which resulted from a cross between *B. rapa* Longyou7 [20], known for its strong cold resistance, and *B. napus*. We have studied the cold resistance mechanisms of osmotic adjustment, enzymatic activity, ROS signal generation, and transmission in 16VHNTS309 from physiological, biochemical, and cellular perspectives [4].

To understand the cold resistance mechanism of *B. napus*, we analyzed the cold-tolerant *B. napus* 16VHNTS309 and weak cold-resistant *B. napus* of Tianyou 2238 through transcriptome sequencing, gene expression, GO, and KEGG pathway profiling at normal temperature (25°C) and under cold treatment (4°C) using the Illumina sequencing technique. Based on differential gene expression and GO and KEGG pathway analysis, genes and metabolic pathways related to ROS production, antioxidant systems, and signal transduction were identified. This study aims to enhance our understanding of the molecular-level cold stress response pathways and identify effective strategies to improve cold tolerance in *B. napus*.

2 Materials and Methods

2.1 Material

Our group has cultivated a cold-tolerant winter *B. rape* variety, Longyou7, which can survive in extremely low temperatures (down to -32°C , with an overwinter survival rate of more than 90%) [20]. To

develop cold-resistant lines of *B. napus*, diploid *B. rapa* Longyou 7 (A_rA_r , $2n = 2x = 20$) was hybridized with amphidiploid *B. napus* Vision ($A_nA_nC_nC_n$, $2n = 4x = 38$) to create the F_1 generation ($A_nA_rC_n$, $2n = 3x = 29$). Although F_1 seeds exhibited heterosis, the rate of self-crossing was very low (0 to 6 seeds per 100 pollinated flowers). After two rounds of self-crossing, F_3 plants were crossed with *B. napus* Vision and backcrossed to *B. napus* Vision. The BC_1F_1 generation seeds were self-crossed three times to obtain BC_1F_4 seeds, which were then subjected to a cold resistance test to select the highly cold-resistant individual plant, 16VHNTS309.

2.2 Cold Stress Treatment

The overwintering rates of strong cold-resistant *B. napus* 16VHNTS309 and weak cold-resistant *B. napus* Tianyou 2238 were 85.38% and 18.95%, respectively, provided by Gansu Provincial Key Laboratory of Crop Genetics and Germplasm Improvement, Gansu Agricultural University. The *B. napus* cultivars 16VHNTS309 and Tianyou 2238 underwent germination in 12×8 hole float trays ($60 \text{ cm} \times 40 \text{ cm} \times 8 \text{ cm}$), with pots containing a 3:1 ratio of nutritional soil to vermiculite. Cultivation occurred in an illumination incubator at standard conditions (25°C , 16-h photoperiod, 6000 Lx light intensity). When plants reached the four-leaf stage, they were segregated into two groups. The control group remained under standard conditions for 48 h, while the test group was subjected to cold stress in a pre-cooling incubator at 4°C for the same duration. This process was replicated three times to ensure reliability. Post-experiment, samples were preserved at -80°C for subsequent transcriptome and biochemical analysis.

2.2.1 Transcriptome Analysis

Total RNA extraction was performed utilizing the Trizol total RNA extractor kit (B511311, Sangon, Shanghai, China). RNA samples from 16VHNTS309 and Tianyou2238 of high quality were forwarded to Sangon Biotech (Shanghai) Co., Ltd. (Shanghai, China) for the construction of libraries using HiSeq XTen sequencers (Illumina, San Diego, CA, USA). The quality of the sequenced data was appraised using FastQC (version 0.11.2). HISAT2 (version 2.0) aligned clean reads to the reference genome (<https://www.genoscope.cns.fr/brassicapapus/>, accessed on 01 November 2024). Statistical evaluations were performed using RSeQC (version 2.6.1), and gene coverage ratios were assessed with BEDTools (version 2.26.0). StringTie (version 1.3.3b) calculated gene expression values. DESeq2 (version 1.12.4) identified DEG, considering genes with a $q\text{-Value} < 0.001$ and $|\text{FoldChange}| > 2$ as significantly expressed. Functional enrichment analysis, which included gene ontology and the Kyoto Encyclopedia of Genes and Genomes, pinpointed DEGs substantially enriched in specific GO terms or metabolic pathways, with a false discovery rate ($q\text{-Value}$) < 0.05 indicating significant alteration. Transcriptome data have been uploaded (SRA data: PRJNA1198720, <https://www.ncbi.nlm.nih.gov/sra/PRJNA1198720>, accessed on 01 November 2024).

2.2.2 Index of H_2S , ABA, VB_6

Following cold exposure, the concentrations of VB_6 and ABA were quantified using a DDS11A digital conductometer (Leici Instrument Factory, Shanghai, China) and enzyme-linked immunosorbent assay according to the kit specifications provided by Cominbio (Suzhou, China). H_2S content was determined following the methodology outlined by Lai et al. [21]. SPSS 19.0 statistical analysis was used to test the different significance of the data, Duncan's method was used to make multiple comparisons between different treatments, and the difference significance between treatment and control was used by t -test, the significance level was set at $p < 0.05$.

2.2.3 qRT-PCR

To confirm the accuracy of RNA-Seq data, we selected 23 DEG for qRT-PCR analysis using the Super Real PreMix Plus (SYBR Green) Kit (TIANGEN) on an Applied BioSystems 7500 Real-Time PCR system (Applied BioSystems, Model No. 401511) (Table 1). We quantified gene expression utilizing the $2^{-\Delta\Delta Ct}$ method, with β -actin as the reference gene. Averages and standard deviations (SD) were calculated from three biological replicates.

Table 1: Primer of qRT-PCR

Gene ID	Forward primers	Reverse primers	Product size (bp)
BnaC03g00280D	ACAACCACATCAACAAGCATAACT	GAAGACCTCGTCGCATCCA	212 bp
BnaAnng00210D	GACCACCACATCAACAAGCATAAC	CCTAATCATCGCCGCACCTT	105 bp
BnaA08g23000D	GGTGTGGTGATTACTGTCTTA	CGCCATCGGTCCAATCTCTA	139 bp
BnaA05g16830D	CGCTATCCTCACCGACATTG	GACTGGCTCAAGAACCTCAAG	160 bp
BnaC09g50680D	ACTATGGACGACTTAGCAGATGAG	CGCAGCAGGAGCAAGAAC	186 bp
BnaC08g09930D	TTCACGGCGGCTGCTAAG	CCATATCTCAGGTCCAGTAGTCTCA	249 bp
BnaAnng27260D	TGGTCGTGTCGCTGCTAAG	TCCACTCGTTGGCTCAATCAG	142 bp
BnaA04g00700D	CGTTCTTGAGGTTAGTAGTGAGGAT	GCTTCATCGCTTCTGCTTCTT	233 bp
BnaC05g48620D	CGCCAAGTGGTCCAACAAC	TGAAGTCAAGAAGGTCAGCAGTT	215 bp
BnaA03g24240D	GGAAACCCAAAGGCAGGAGAA	TGTTGGCAGCAGAGTAAGAATACC	157 bp
BnaA03g50710D	TTCTGCTCTTCTCTTCTTCCTC	CTGCCATCCTTGCTGTTCTTAC	214 bp
BnaA08g10870D	AACTCTGGTGCTCCTGTATGG	TGGCTCCTCTTGCGTGAA	151 bp
BnaA06g05150D	CAGGAAGGAGACGGTGTGA	GTGATTGTGAAGGTGGCAGTT	233 bp
BnaC03g09940D	CAGGAGACGGAGGATGTATGC	GGCGGAGGAAGGTGAGAAG	249 bp
BnaA03g22610D	GGAGAGATTCTGCTTCGGAGTATT	GACCAACTTCAACAACCTTCACAA	187 bp
BnaC09g40380D	GGCTCTTCTGATGATGCTATGGT	TCGTGGAGAATATCCTTGGACAAC	128 bp
BnaC05g06430D	CAGGAAGGAGACGGTGTGA	GTGATTGTGAAGGTGGCAGTT	233 bp
BnaC03g16120D	ATGCTTCTGCTTCAATAACG	AAGTCTGTTTCGCTTGTATGC	219 bp
BnaC09g50920D	CGCCGTCCTAAGCCACAA	ATCCATCGCCACCAGATTCAG	124 bp
BnaA02g17550D	CTACGAGAACATAGCCAAGAAGTG	CTGCTGCGTCTTTGAACTACAT	217 bp
BnaA02g37060D	TACGGCAGCAGAAGTTGAAGT	GCATTTGGATGGAAGACACCTAAAG	228 bp
BnaA02g02470D	GGACTACCAAGGAGACCAGAAG	AGAGAAGAATCAGTGGCGACTT	168 bp
BnaA09g07330D	ACCTTCACCACCTTGACGAAT	TGGATGCTTGCTAACGCCTTA	242 bp

3 Results

From the cDNA libraries of 16VHNTS309 and Tianyou2238, we generated high-quality reads, resulting in the creation of 12 libraries. Each library generated approximately 7.55×10^7 raw reads, with a total of 9.06×10^8 raw reads. The Q20 ratios (sequencing error rate <1%) were between 97.13% and 98.49%, and the Q30 ratios (sequencing error rate <0.1%) ranged from 92.75% to 95.96%, reflecting high sequencing quality with a GC content above 47% (Table A1). We utilized trimmomatic software for data preprocessing, which eliminated low-quality reads, yielding 8.77×10^8 clean reads. The mean number of clean reads per library was 7.31×10^7 . The Q30 ratio exceeded 92% across all libraries, maintaining a consistent GC content of about 47%. Furthermore, 91% of the clean reads successfully aligned with the *B. napus* reference genome. The high correlation coefficients (r) nearing 1 and consistent gene expression density curves across samples confirmed the test's reliability and the suitability of the sample selection.

To investigate gene expression differences in response to cold stress between the cold-tolerant 16VHNTS309 and the weak cold-resistant Tianyou2238, DEGs (q-Value < 0.05 and log2-fold-change > 2) were determined in both strains. The inter-sample correlation heatmap confirmed the high reliability of repeated data (Fig. 1A). Statistical analysis of gene expression density distribution helped in assessing the

levels of differential gene expression in 16VHNTS309 and Tianyou2238 over various treatment periods (Fig. 1B). The expression patterns of DEGs in both strains were consistent through various low temperature treatment durations. A Venn diagram displayed the regulation patterns of DEGs, showing up- and down-regulation in both winter rapeseed varieties under cold stress. After 48 h of cold exposure, 6127 DEGs (3427 up-regulated and 2700 down-regulated) in 16VHNTS309 and 8531 DEGs (4738 up-regulated and 3793 down-regulated) in Tianyou2238 were identified (Fig. 2). The higher number of up-regulated DEGs indicates a complex and varied response mechanism in *B.napus* of both 16VHNTS309 and Tianyou2238.

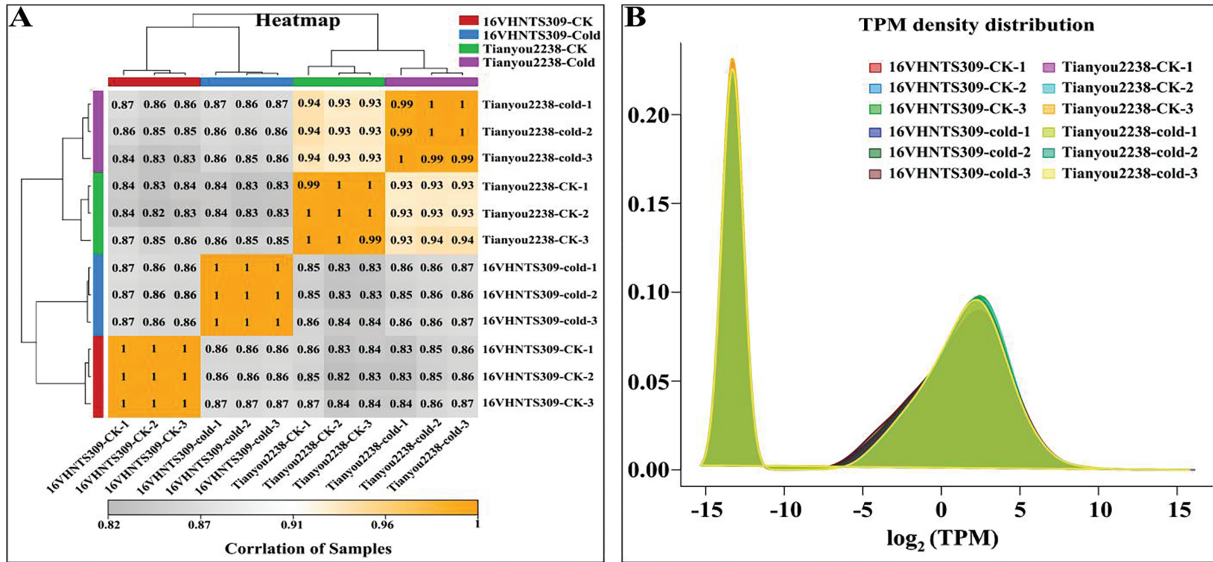


Figure 1: A: Heat-map of correlation analysis between samples. B: Curve graph of gene expression density

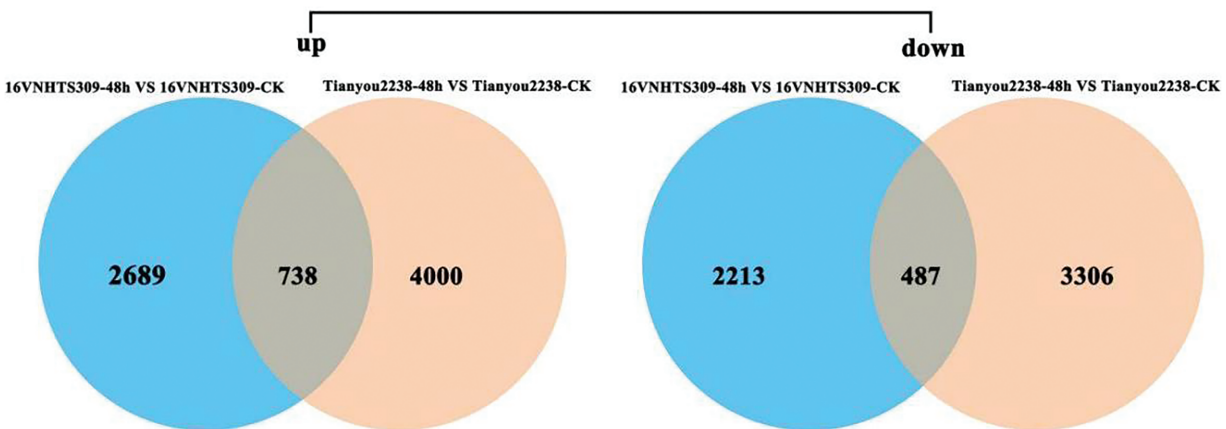


Figure 2: List of DEGs and ADEGs in different treatment

3.1 qRT-PCR Analysis

Following cold stress treatment, 23 DEGs from *B. napus* cultivars 16VHNTS309 and Tianyou 2238 underwent qRT-PCR analysis (Fig. 3) to corroborate the transcriptome sequencing findings. The expression

patterns of these DEGs in the qRT-PCR confirmed those observed in the RNA-Seq analysis, substantiating the sequencing results' reliability and demonstrating RNA-Seq's capability to accurately reflect the transcription levels of *B. napus* 16VHNTS309 and Tianyou 2238 under cold conditions.

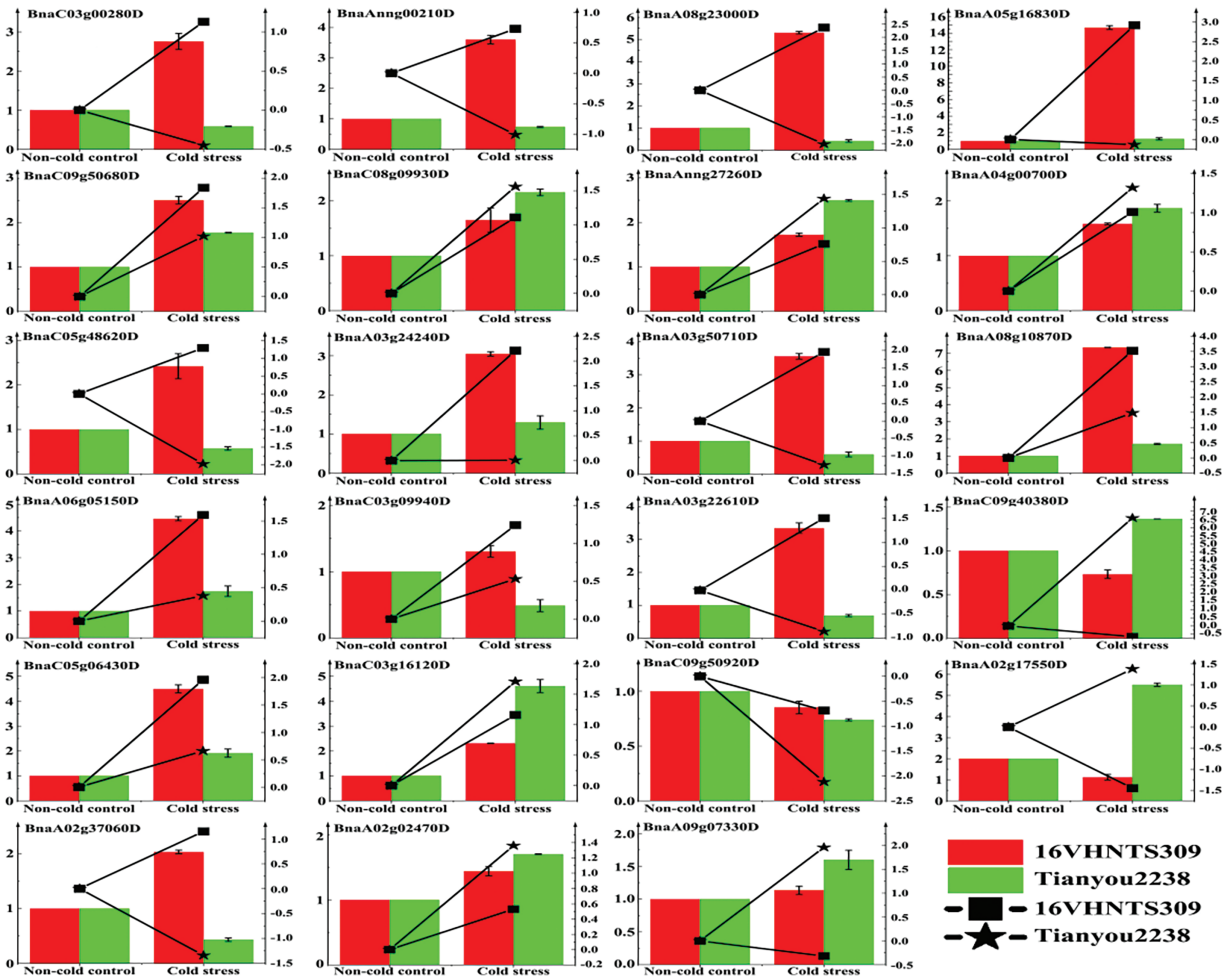


Figure 3: Post 48 h of cold exposure at 4°C, 23 DEGs from *B. napus* 16VHNTS309 and Tianyou 2238 were subjected to qRT-PCR. Error bars represent the standard errors of the mean values of relative expression levels measured by qRT-PCR (left y-axis). Dashed lines illustrate the changes in transcript levels (log₂-fold) based on the FPKM values from RNA-Seq (right y-axis)

3.2 Go Analysis

GO analysis was conducted to identify the genes differentially expressed under cold stress in *B. napus* 16VHNTS309 and Tianyou 2238. This analysis segregated the DEGs into three principal functional categories: molecular function (MF), biological process (BP), and cellular component (CC). DEGs in CC were predominantly found in extracellular regions (GO: 0005576) and others (refer to Table A2). MF DEGs primarily showed enrichment in functions such as oxidoreductase activity (GO: 0016491), catalytic activity (GO: 0003824), and iron ion binding (GO: 0005506). BP DEGs were chiefly involved in alpha-amino acid metabolism (GO: 1901605), oxidation-reduction processes (GO: 0055114), and small molecule metabolism (GO: 0044281).

Conversely, in the weak cold-resistant *B. napus* Tianyou 2238, DEGs in MF categories included structural constituent of ribosome (GO: 0003735) and structural molecule activity (GO: 0005198). CC DEGs were largely concentrated in the ribosome (GO: 0005840) and ribonucleoprotein complex (GO: 1990904), while BP DEGs were mainly involved in translation (GO: 0006412) and peptide biosynthetic processes (GO: 0043043) (Table A3). These findings underscore the distinct roles of genes from 16HNTS309 and 2238 in GO enrichment under cold stress, playing essential roles in ROS production and clearance processes in both BP and MF of cold-resistant *B. napus*.

3.3 KEGG Analysis

Post-cold stress, there were notable changes in 57 pathways (q-Value <0.05) in the cold-resistant *B. napus* of 16VHNTS309 (Table A4), as opposed to only 9 pathways in the weak cold-resistant Tianyou 2238 (Table A5). These observations indicate that 16VHNTS309 employs a more intricate mechanism of cold resistance compared to Tianyou 2238. DEGs in 16VHNTS309 were significantly enriched in pathways such as carbon metabolism (Ko, 01200), biosynthesis of amino acids (Ko, 01230), glyoxylate and dicarboxylate metabolism (Ko, 00630), and sulfur metabolism (Ko, 00920) (Fig. 4a). During cold stress, DEGs in Tianyou 2238 were prominently enriched in the ribosome (Ko, 03010), biosynthesis of amino acids (Ko, 01230), and sulfur metabolism (Ko, 00920) (Fig. 4b).

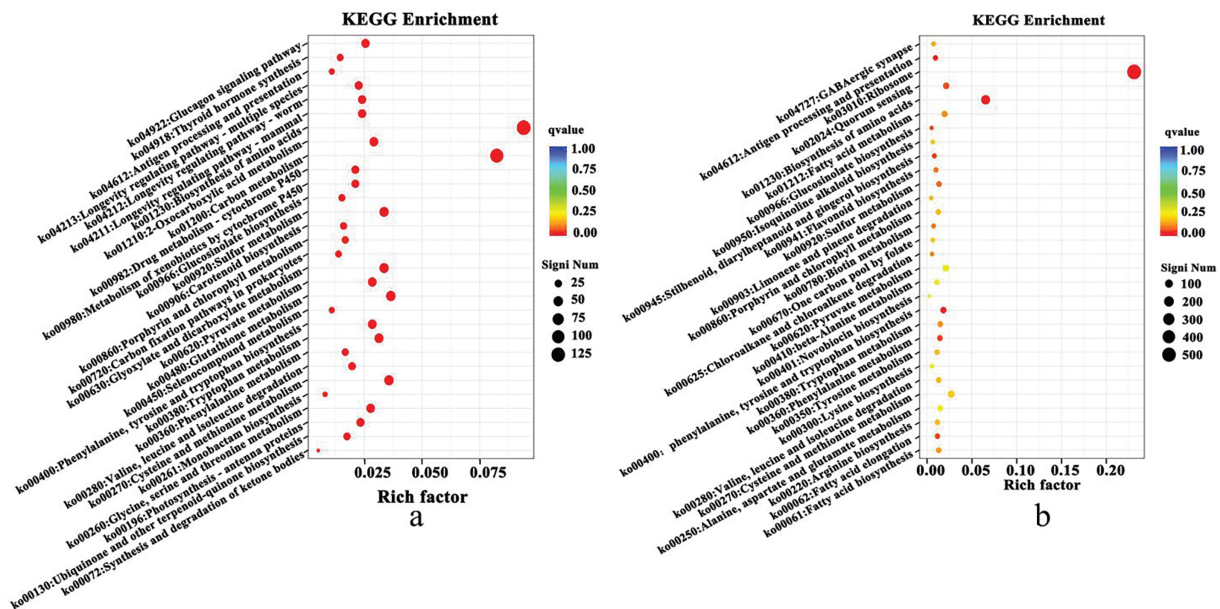


Figure 4: KEGG enriched DEGs in 16VHNTS309 (a) and Tianyou2238 (b) at 48 h of cold stress

3.4 Physiological Index Analysis

There were significant differences in ABA, VB_6 , and H_2S contents among varieties under cold stress. Our study indicated that ABA content in 16VHNTS309 was 377.16 $\mu\text{g/L}$, significantly higher than in Tianyou2238 (Fig. 5A). The H_2S content in the cold tolerant 16VHNTS309 was 11.59 nmol/g, significantly higher than in Tianyou 2238 (Fig. 5B). The VB_6 content in 16VHNTS309 was measured at 22.14 $\mu\text{g/g}$, significantly higher than in Tianyou 2238 (Fig. 5C), suggesting that the cold-tolerant *B. napus* 16VHNTS309 accumulate more VB_6 .

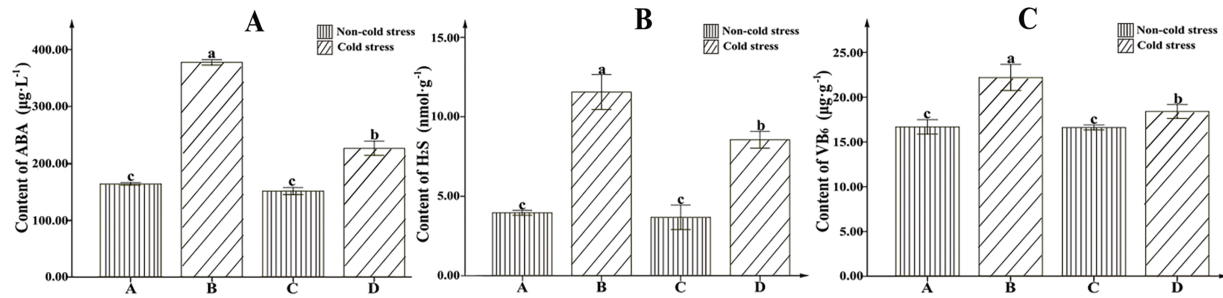


Figure 5: The activity of ABA (A), H₂S (B), and VB₆ (C) content accumulation in parts of 16VHNTS309 and Tianyou2238 under cold stress at 4°C for 48 h. Uppercase letters denote a significant difference ($p < 0.05$) in the data between cold-stressed samples and controls

4 Discussion

4.1 Synthesis of Vitamin B₆ in *B. napus* and Its Role in ROS Elimination

VB₆ plays a pivotal role in plant stress responses. VB₆ demonstrates significant antioxidant capabilities, effectively mitigating ROS accumulation in response to diverse environmental stresses [22]. VB₆ synthesis in plants predominantly occurs through the DXP-independent pathway, with the critical genes, *PDX1* [23] and *PDX2* [24], identified in *C. nicotiana*. These genes are essential for PLP synthase activity; *PDX2* catalyzes the production of NH₃ from glutamine, while *PDX1* facilitates the conversion of glyceraldehyde 3-phosphate, ribose 5-phosphate, and NH₃ into PLP [25,26]. Chen et al. [27] isolated a *PDX1* homolog, *PDX1.3*, from yeast under drought and salt stress, with further studies confirming its critical role in biological responses. The expression of *PDX1* and *PDX2* is up-regulated in *Arabidopsis thaliana* under abiotic stress [28], leading to increased VB₆ content and enhanced antioxidant activity when PDX proteins are overexpressed [29]. Under the cold stress, the VB₆ content in 16VHNTS309 was significantly higher than in Tianyou 2238 (Fig. 5C), suggesting that the cold-tolerant *B. napus* 16VHNTS309 accumulates more VB₆, which aids in reducing ROS production. This difference may stem from the distinct VB₆ metabolic pathway in response to cold stress between 16VHNTS309 and Tianyou2238. Transcriptome data indicated that *PDX1* plays a vital role in regulating PLP synthesis (EC:4.3.3.6), with genes such as BnaC03g00280, BnaAnng00210D, BnaC04g45760D, BnaA10g13320D being up-regulated in 16VHNTS309 following cold stress, but not in Tianyou 2238 (Fig. 6). Consequently, 16VHNTS309 synthesizes more PLP, whereas Tianyou 2238 does not exhibit similar gene expression levels. VB₆ is synthesized from PLP via the action of PL phosphatase (EC:3.1.3.74), during which the gene BnaA08g23000D is up-regulated in 16VHNTS309 but down-regulated in Tianyou 2238 by a factor of 2.02. Overall, several genes are up-regulated in the cold-tolerant *B. napus* 16VHNTS309 under cold stress, unlike in Tianyou 2238, indicating that 16VHNTS309's cold resistance is linked to the VB₆ metabolic pathway, which plays a beneficial role in eliminating excessive ROS *in vivo*. These results further confirm that *PDX1* expression is up-regulated under various stresses, significantly contributing to VB₆ synthesis and actively regulating plant stress resistance [30].

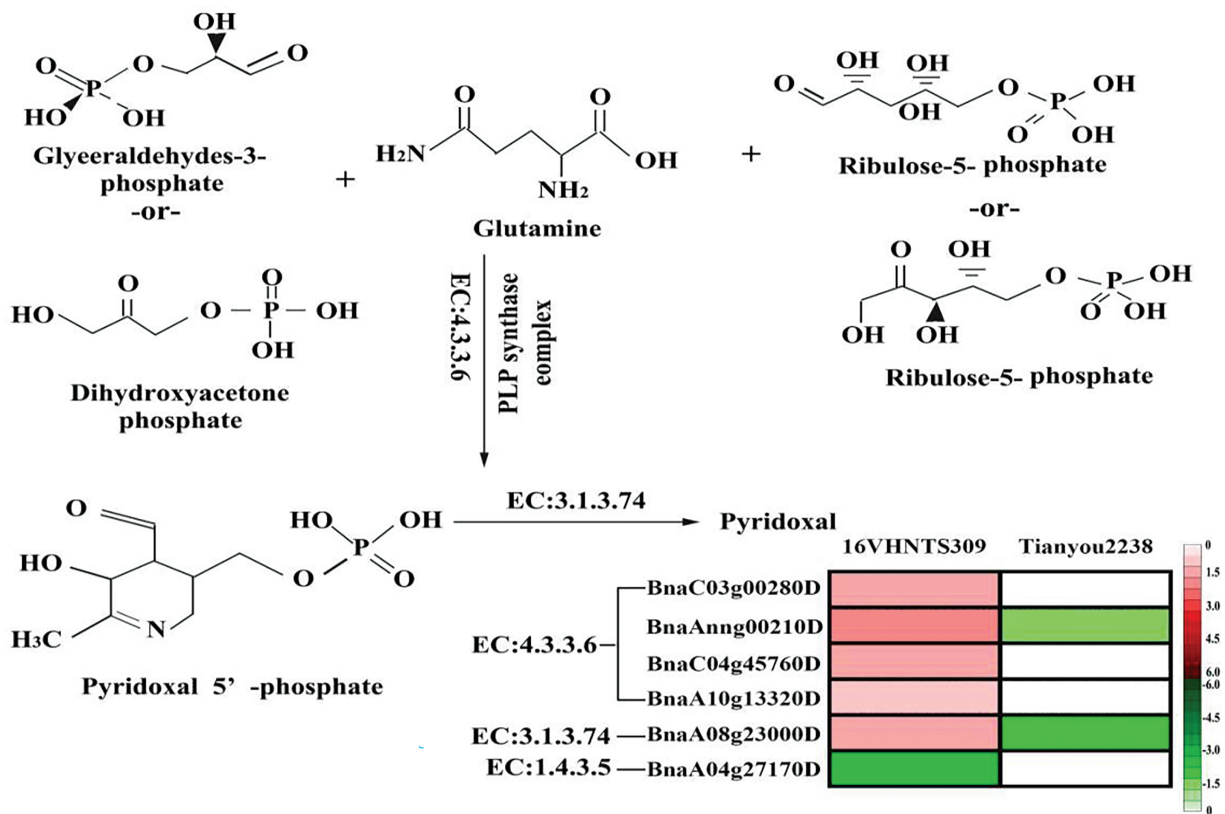


Figure 6: *B. napus* of DEGs in VB₆ pathway, which biosynthetic pathways was quoted from Huang et al. [30]

4.2 Role of Peroxisome in Maintaining ROS Balance in *B. napus*

Peroxisomes are crucial for plant development, playing a significant role in controlling H₂O₂ levels within the ROS scavenging system [31,32]. Immature peroxidase precursors are synthesized in the endoplasmic reticulum. These precursors are then assembled into complete peroxidases by PMP, matrix protein, and PEX. PMP, containing a peroxisomal membrane targeting signal (mPTS), is synthesized at the ribosome and directed into the endoplasmic reticulum by mPTS, mediated by PEX3 and PEX19 [33]. The peroxidase precursors then form complexes with the matrix proteins PTS1-PEX5 and PTS2-PEX7, which are recognized by PEX14 and PEX13 on the membrane, respectively, and enter the peroxisome Matrix [34]. The complexes dissociate, releasing the matrix proteins into the matrix, while empty PEX5 and PEX7 are transferred out of the peroxisome by the translocation complexes (PEX1, PEX10, PEX12) for subsequent transfer [35,36]. Studies have highlighted that the PTS1-PEX5 complex plays a critical role in peroxisome formation [37]. Results indicated that PTS1 genes of BnaC03g09940D, BnaC03g26640D, BnaA03g22610D, BnaC01g36930D, BnaA01g29410D, BnaA05g25050D, BnaC05g39220D were up-regulated in the cold-tolerant *B. napus* 16VHNTS309 (Fig. 7). In contrast, the expression of PTS1-PEX5 genes was down-regulated or absent in the weakly cold-resistant *B. napus* Tianyou2238, suggesting that the PEX5-PTS1 complex is vital for peroxisome synthesis under cold stress (Fig. 7).

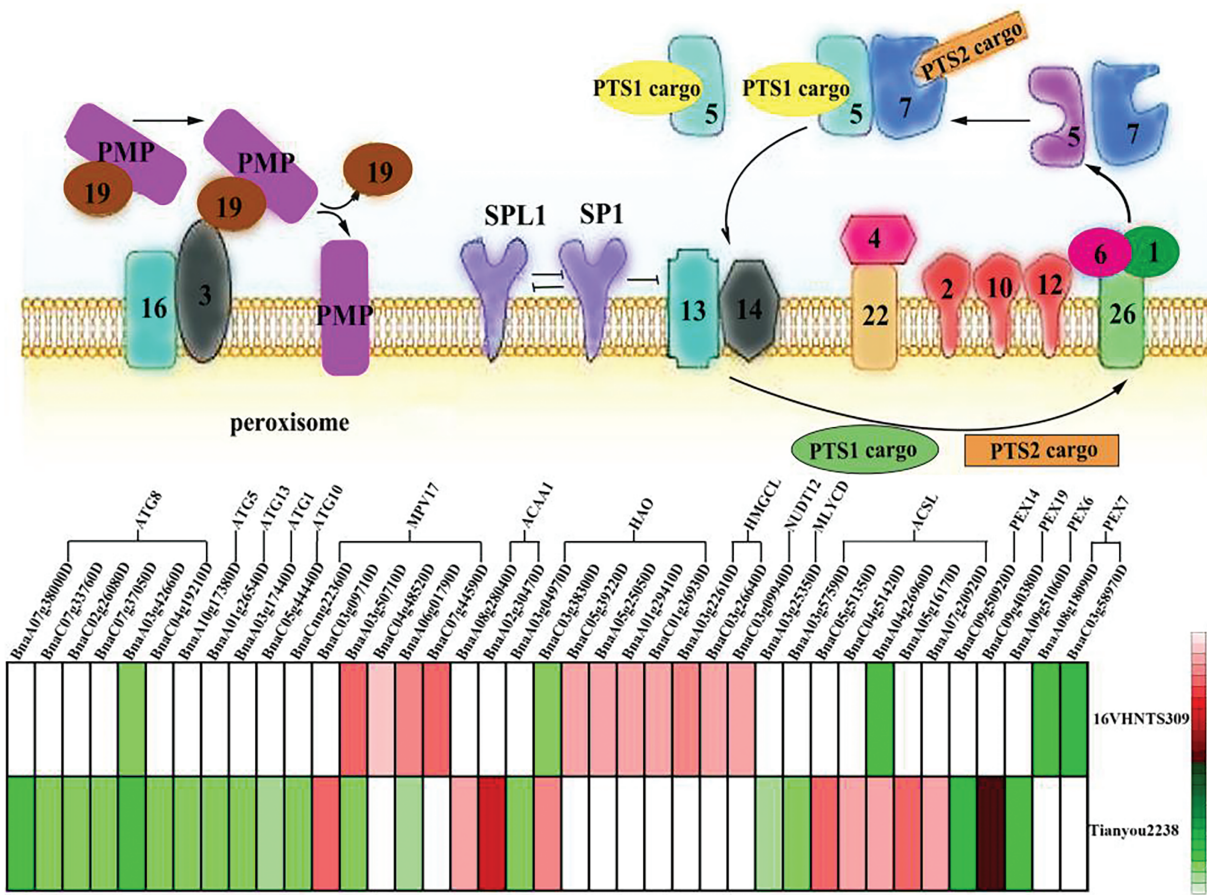


Figure 7: Peroxisomal metabolic pathway quoted from Pan et al. [34]: Analysis of peroxisomal metabolic and autophagosome pathway in *B.napus*

Mano et al. [38] reported that PTS1-PEX5 could be recognized by Pex14, and regulating the expression of the *PEX14* gene enables *Arabidopsis thaliana* to respond actively to drought stress, ROS metabolism, and metabolic homeostasis. However, the gene BnaC09g50920D regulating *PEX14* in the weak cold-resistant *B.napus* Tianyou2238 was down-regulated by 2.13 following cold stress, indicating a reduced capability of *PEX14* to identify and transport PEX5-PTS1. The PEX1-PEX6 complex then interacts with the ubiquitinated PEX5, which is released into the cytoplasm [39]. In *Arabidopsis thaliana*, mutations in *PEX6* or *PEX26* have been shown to decrease *PEX5* output, further indicating that the stability of the PEX1, PEX6, and PEX26 complexes impacts the stability and function of peroxisomes [40]. Our study showed that the *PEX6* gene BnaA09g51060D was down-regulated in the weak cold-resistant *B.napus* of Tianyou2238, affecting the stability and output capacity of the PEX1, PEX6, and PEX26 complex (Fig. 7).

These findings demonstrate that cellular ROS can regulate PEX gene expression and ultimately influence the increase in peroxisome numbers. Analysis of the peroxidase formation process shows that the control of PEX14 and PEX5 input and output, and related PEX6 genes in the weak cold-resistant *B. napus* Tianyou2238 were down-regulated, which indicates a reduction in peroxisome production in Tianyou2238 cells, thereby diminishing cold adaptability. It is hypothesized that peroxidase synthesis inhibition is the primary reason for Tianyou2238's poor cold resistance. The study also confirmed that redundant or damaged peroxisomes could be degraded by autophagosomes following environmental stress [37]. Plant autophagy, regulated by *ATG* genes, was shown by Ren et al. [41] to be up-regulated in *Arabidopsis thaliana* following aluminum

ion stress; autophagy mutants suffered significant oxidative damage. For example, *Arabidopsis* *ATG2*, *ATG7*, and *ATG18* mutants exhibited peroxisome aggregation [42]. Under cold stress, numerous autophagosome genes (*ATG1*, *ATG5*, *ATG8*, *ATG10*, and *ATG13*) were down-regulated in weakly cold-resistant *B. napus* Tianyou2238, indicating an impaired capacity to clear redundant or damaged peroxisomes.

4.3 Effects of Sulfur Metabolism on ROS Scavenging Mechanism in Cold-Resistant *B. napus*

Previous studies have shown that the absorption, transport, and assimilation of sulfur compounds—including free sulfur (S_0), hydrogen sulfide (H_2S), glutathione (GSH), and phytochelatins (PCs)—influence plant growth, development, and stress tolerance to varying degrees. Studies reported that aging plants exhibit lower H_2S levels but higher malondialdehyde (MDA) levels, suggesting a negative correlation between H_2S and MDA levels [43]. Moderate H_2S levels enhance the activity of antioxidant enzymes such as superoxide dismutase (SOD), ascorbate peroxidase (APX), peroxidase (POD), and catalase (CAT), thereby enhancing the plants' antioxidant capacity to remove more ROS. For example, exogenous H_2S application has been shown to delay senescence in Chinese rose, *Euonymus bungeana*, mountain wood, and pomegranate bark [44]. Our results indicate that the H_2S content in the cold-tolerant 16VHNTS309 was significantly higher than in Tianyou 2238. Additionally, MDA levels were significantly higher in Tianyou2238 than in 16VHNTS309 [4], further supporting the inverse relationship between H_2S and MDA content proposed by Yu et al. [43].

Transcriptome data reveal that the sulfur metabolism pathway plays a crucial role in *B. napus* under cold stress. Key genes encoding ATP sulfurylases have been cloned in *Arabidopsis thaliana* [45], and *Brassica* [46]. ATP sulfurylases (EC 2.7.7.4) catalyze the conversion of SO_4^{2-} into adenosine 5'-phosphosulfate (APS) [47]. Our findings show that seven genes encoding ATP sulfurylases were upregulated in 16VHNTS309, whereas only Bna05g15510D was upregulated, and BnaA06g36560D and Bna07g17320D were downregulated in Tianyou2238. This suggests that the cold-resistant *B. napus* 16VHNTS309 exhibits enhanced catalytic activity of ATP sulfurylases, converting SO_4^{2-} to APS. Subsequently, APS is reduced to SO_3^{2-} by APS reductase (APR, EC 1.8.99.2) [48]. Our study found that genes encoding APS reductase in 16VHNTS309 (Fig. 8), specifically BnaC07g37060D, BnaA03g59800D, BnaA01g11840D, BnaC04g19270D, BnaA03g45080D, and BnaC01g13420D, were upregulated, indicating a robust capacity to produce SO_3^{2-} . Conversely, these genes were downregulated in Tianyou2238. Sulfite is further reduced to H_2S by sulfite reductase (SIR, EC 1.8.7.1), with genes encoding SIR upregulated in 16VHNTS309 but not significantly expressed in Tianyou 2238. This demonstrates that the sulfur metabolism pathway undergoes significant alterations under cold stress in 16VHNTS309, resulting in increased H_2S production. Research also indicates that H_2S plays a critical role in the antioxidant enzyme system and in the accumulation of osmotic regulatory substances under stress [49].

Cysteine (Cys) synthesis occurs through the action of serine acetyltransferase (SAT, EC: 2.3.1.30) and O-acetylserine (thiol) lyase (OASTL, EC: 2.5.1.47), utilizing H_2S and O-acetylserine (OAS). As a central hub in sulfur nutrient metabolism, Cys serves not only as a sulfur donor for vitamins and coenzymes but also as a substrate for the synthesis of the antioxidant GSH [50]. GSH effectively scavenges H_2O_2 in plants, underscoring Cys's vital role in oxidative stress mitigation [51]. The present study revealed that numerous cysteine synthetase genes, including those for SAT and OASTL, were upregulated in both 16VHNTS309 and Tianyou 2238, enhancing Cys synthesis in *B. napus* under cold stress. However, compared to 16VHNTS309, Tianyou 2238 exhibited lower H_2S levels and Cys synthesis gene expression after cold exposure. It is speculated that 16VHNTS309, with its strong cold resistance, possesses superior abilities to absorb, transport, and assimilate sulfur elements, subsequently accumulating more Cys for use as sulfur donors for vitamins, coenzyme factors, and GSH.

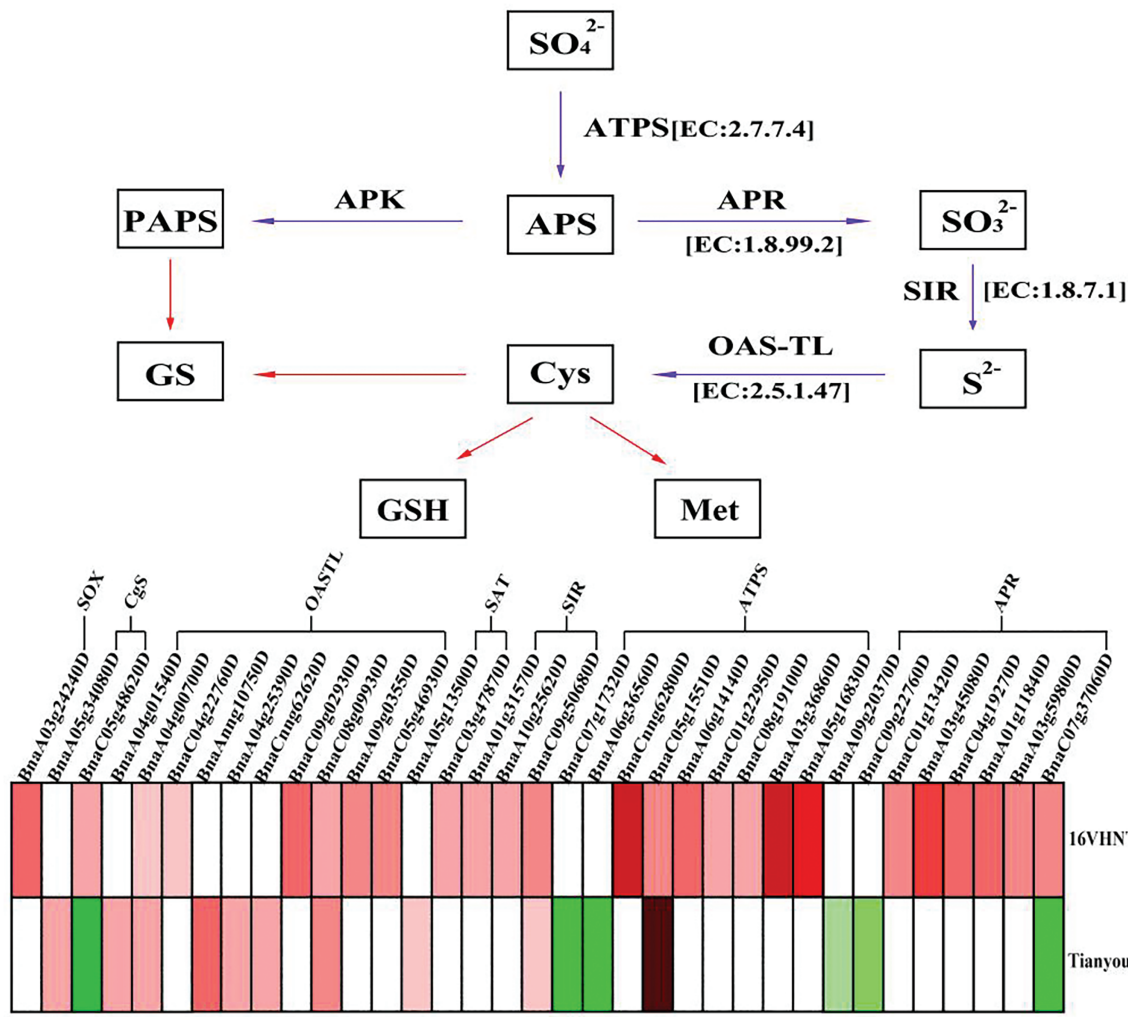


Figure 8: Analysis of sulfur metabolism in *B.napus* [52]

4.4 The Changes of SOD and CAT Activities in *B.napus* Are Actively Involved in Regulating ROS Metabolism

An appropriate level of ROS is crucial for the normal growth and development of plants, reliant on a balance between ROS production and elimination. Plants with enhanced cold resistance exhibit higher activities of antioxidant enzymes, which are integral in managing ROS metabolism and mitigating membrane lipid peroxidation. This observation is well-supported in various crops including wheat [53] and rice [54]. The activities of catalase (CAT), peroxidase (POD), and superoxide dismutase (SOD) in the cold-resistant 16VHNTS309 were significantly greater than in Tianyou2238 [4]. Transcriptome analysis revealed that the expression of SOD genes Bna05g06430D, BnaA06g05150D, and BnaA01g14450D was up-regulated in 16VHNTS309, but not in Tianyou2238. Additionally, BnaA08g10870D, BnaC03g65530D, BnaC07g45360D, and BnaA03g53180D showed increased expression levels of 3.52, 3.45, 3.03, and 2.61, respectively, in 16VHNTS309. In contrast, BnaC07g45360D and BnaA03g53180D were not significantly expressed in Tianyou2238. The sulfur metabolism pathway further demonstrated that the cold-resistant 16VHNTS309 could synthesize more Cys and promote the synthesis of GSH (Fig. 8). Our findings indicate

that minimal ROS accumulated in 16VHNTS309 [4]. The main reason is that the activities of CAT, SOD, and GSH are crucial in reducing ROS production in 16VHNTS309.

4.5 The Strong Cold Resistance of *B.napus* Was Correlated with the Interaction of ROS and Ca²⁺ Signals

Ca²⁺ concentration increases in plants following cold stress. NADPH oxidase is a pivotal enzyme for ROS production, while mutations in RBOHD/F can inhibit the accumulation of both ROS and Ca²⁺ in cells [55]. This is because Ca²⁺ binds to the Ca²⁺ site on NADPH oxidase, altering its conformation and triggering ROS production. Our studies confirm that ROS is mediated by NADPH in *B.napus* during cold stress [4]. Studies on *Arabidopsis thaliana* have shown that the expression of calmodulin (CaM), a Ca²⁺ signaling receptor, increases under cold stress, highlighting the significant role of the CaM protein in plant adaptation to low temperatures [56]. Transcriptome results indicated that several genes encoding CaM and Calcineurin B-like proteins (CBLs) were significantly up-regulated in 16VHNTS309. However, these genes were either down-regulated or not significantly expressed in Tianyou2238, except for BnaA09g03360D and BnaA06g19660D (Fig. 9). This suggests that the Ca²⁺ signaling pathway plays a crucial role in the strong cold resistance of *B.napus* 16VHNTS309. It is hypothesized that Ca²⁺ combines with NADPH, inducing a ROS wave that couples to form a rapid signaling system capable of transmitting signals to neighboring and distal cells.

4.6 The Strong Cold Resistance of *B.napus* Interacted with ROS, MAPK, and WRKY

Under stress conditions, increased ROS production in plants leads to the activation of Ca²⁺ signaling channels and the accumulation of phospholipid acid (PA) [57,58]. The accumulated PA and Ca²⁺ are vital for activating the serine/threonine protein kinase (OXI1), which in turn activates the MAPK cascade (MAPK3/6) [59], thereby influencing plant stress resistance. Thus, the MAPK cascade response plays a crucial role in signal reception, transduction, and nuclear transmission within the signal transduction pathway [59], and it regulates the expression of relevant stress-resistant genes. It has been reported that MKP2, closely associated with oxidative stress signaling in *Arabidopsis*, actively regulates MAPK3/6 activation and the oxidative stress response in cells [60]. Current results show that the MAPK3/6 gene BnaC03g55440D was down-regulated by 1.01, and the MAPK3/6 related MKP2 and key gene BnaC05g45710D were down-regulated by 2.78 in Tianyou 2238 following cold stress. However, BnaC05g45710D was up-regulated by 1.78 in *B.napus* 16VHNTS309 (Fig. 9), indicating that MKP2 is actively involved in regulating MAPK3/6 activation, thereby affecting the stress resistance of *B.napus*.

Increasing evidence suggests that ROS can enhance transcription factor expression, which then regulates the expression of stress-responsive genes to improve plant stress resistance [61]. Among these, the transcription factor WRKY is one of the largest transcription families in plants and is involved in various stress response regulatory pathways [62]. For example, the up-regulation of WRKY33 in *Arabidopsis* directs phosphorylation targeting MAPK3/6, enhancing plant stress resistance [63]. Our study revealed that several genes (BnaCnng66020, BnaA05g34850D, BnaA03g17820D, BnaC04g06800D, BnaC03g21360D) of WRKY33 were up-regulated in 16VHNTS309 after cold stress, while the same genes BnaCnng66020D, BnaA03g17820D, BnaC03g21360D were down-regulated in Tianyou2238 (Fig. 9). This suggests that WRKY33 plays a significant role in the cold tolerance of 16VHNTS309. It is further suggested that the up-regulated expression of WRKY33 may interact with MAPK3/6 to enhance the cold tolerance of 16VHNTS309.

Studies also indicate that cold tolerance in *Arabidopsis thaliana* is associated with the up-regulated expression of AtWRKY22, AtWRKY33, and AtWRKY25 [64]. Up-regulation of WRKY22 in wheat and oil

palm [65] has been shown to confer significant cold resistance. Our study found that the gene (BnaCnng02000D) of WRKY22 and genes (BnaC03g16740 and BnaA03g13820D) of WRKY25 were up-regulated in 16VHNTS309, whereas the same genes of WRKY22 and WRKY25 were not significantly expressed or were down-regulated, respectively. Based on these findings, it is suggested that the cold tolerance of *B.napus* 16VHNTS309 is related to the up-regulated expression of WRKY22, WRKY33, and WRKY25 (Fig. 9).

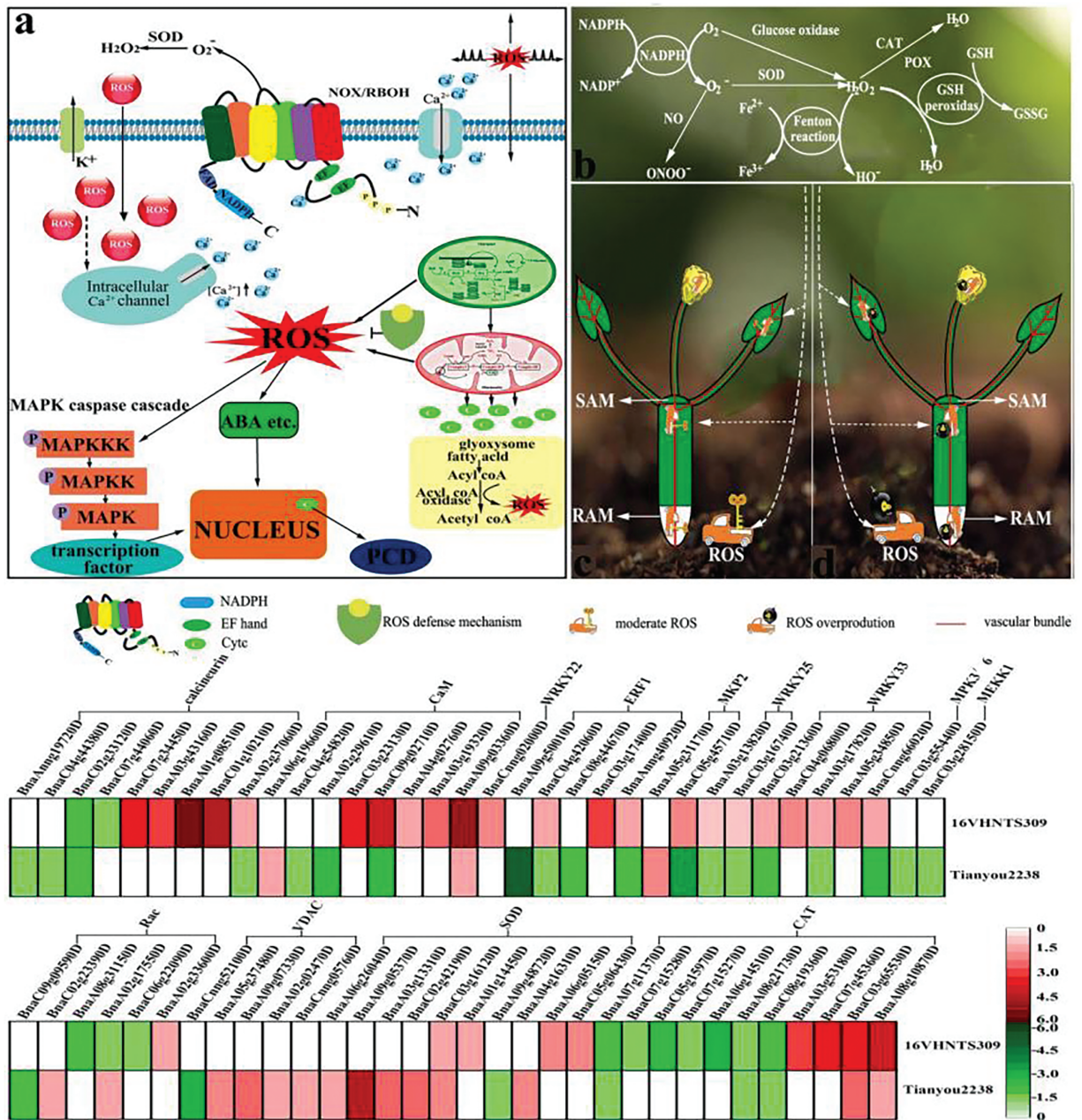


Figure 9: Signal transduction mechanism of ROS in *B.napus*. These mechanisms include ROS production, ROS clearance, the MAPK cascade, Ca^{2+} signaling, and VDAC protein, etc. (a), (b): ROS generation and scavenging was quoted from Zhang et al. [66], (c): When the ROS content in the plant is lower than the “threshold”, ROS (like a key) will be conducive to the growth and development of plants. (d): Conversely, an imbalance in ROS homeostasis can lead to oxidative explosions, detrimental to plant growth and development

4.7 The Strong Cold Resistance of *B. napus* Was Correlated with ROS, ABA, and H₂S Interactions

ROS also interact with other signaling molecules, forming complex networks that enable plants to effectively respond to chilling injuries, high temperatures, and other stresses. Advances in genetics, molecular biology, biochemistry, and cytology have established that stomatal closure is regulated by ROS and ABA. Studies, including one by Singh et al. [67], have shown that DPI can inhibit ROS production from NADPH oxidase. When treated with DPI for 30 min, ROS fluorescence in stomatal guard cells significantly decreased, and the stomatal closure process was markedly inhibited. This evidence supports the interactions between ROS and ABA in stomatal regulation. The role of ABA in stomatal closure has been extensively studied; PYR/PYL/PCAR are identified as ABA signal receptors in guard cells. Stress treatment inhibits the activity of the PP2C enzyme and changes the conformation of activated PYLs. The interaction between PYLs and PP2C regulates the protein kinase OST1, which is crucial for activating the NADPH enzyme, promoting ROS production, calcium influx, anion outflow, and ultimately stomatal closure (Fig. 10). Our study indicated that ABA content in 16VHNTS309 was significantly higher than in Tianyou2238, suggesting that ABA accumulation aids stomatal closure in *B. napus* under low-temperature stress, aligning with prior studies. Transcriptome data revealed that genes BnaA10g00540D and Bna04g47050D encoding the PYR/PYL receptors were up-regulated in 16VHNTS309, while 13 receptor genes were down-regulated in Tianyou2238 after cold stress. This resulted in a significant change in the conformation of ABA receptors in 16VHNTS309 cells, activating downstream signals from PP2C and SNRK2, and enhancing ABA accumulation. Additionally, genes BnaC05g41830D, BnaA05g27660D (PP2C), and BnaA06g22800D, BnaC03g50700D, BnaC06g20490D (SNRK2) were up-regulated in 16VHNTS309, but not significantly expressed in Tianyou2238. These physiological, cytological, and transcriptomic findings demonstrate that ABA plays an active role in regulating stomatal closure and cold adaptation in the highly cold-resistant *B. napus* 16VHNTS309. Under stressful conditions, H₂S accumulates and contributes to ABA-induced stomatal closure. Our results show that the sulfur metabolism pathway in 16VHNTS309 is crucial, with significantly higher H₂S levels than in Tianyou2238, indicating that the synergy between H₂S and ABA is a key mechanism of cold stress response in *B. napus*.

4.8 Excessive ROS Can Induce Up-Regulation of VDAC Expression, and Then Trigger PCD

Mitochondrial pore protein (VDAC) has been identified as a key molecule in mitochondrial-mediated PCD. Reduced VDAC expression leads to a 4-fold decrease in ATP synthesis [68], while VDAC knockout directly affects cell metabolism and normal function [69]. VDAC, located in the outer mitochondrial membrane, acts as a “gatekeeper” for metabolite transport between the mitochondria and cytoplasm [70] and is also thought to mediate ROS release into the cytoplasm [69]. Abiotic stresses such as cold, drought, and saline-alkali conditions induce ROS production, with varying VDAC gene expressions reported under these stresses [71]. Studies have also shown that apoptosis is often accompanied by increased ROS production and upregulated VDAC expression, resulting in the VDAC channel switching to a closed state. Our results indicated that cold stress resulted in the relative electrical conductivity of weak cold-resistant *B. napus* 2238 being significantly higher than that of strong cold-resistant *B. napus* 16VHNTS309, suggesting a higher frequency of VDAC channel closure in Tianyou2238. qRT-PCR results showed that overexpression of VDAC1 reduced the cold tolerance of *Arabidopsis thaliana*, and VDAC1 mutant strains performed better than wild-type plants under cold stress, indicating a negative regulatory role for VDAC1 in cold stress response [72]. The current study showed that genes BnaCnng05760D, BnaA02g02470D, BnaA09g07330D, and BnaA05g37480D were up-regulated by 1.35, 1.37, 1.97, and 1.57, respectively. BnaCnng52100D was down-regulated by 2.78, confirming that weak cold-resistant *B. napus* 2238 accumulated more ROS, leading to enhanced membrane lipid peroxidation and changes in membrane permeability.

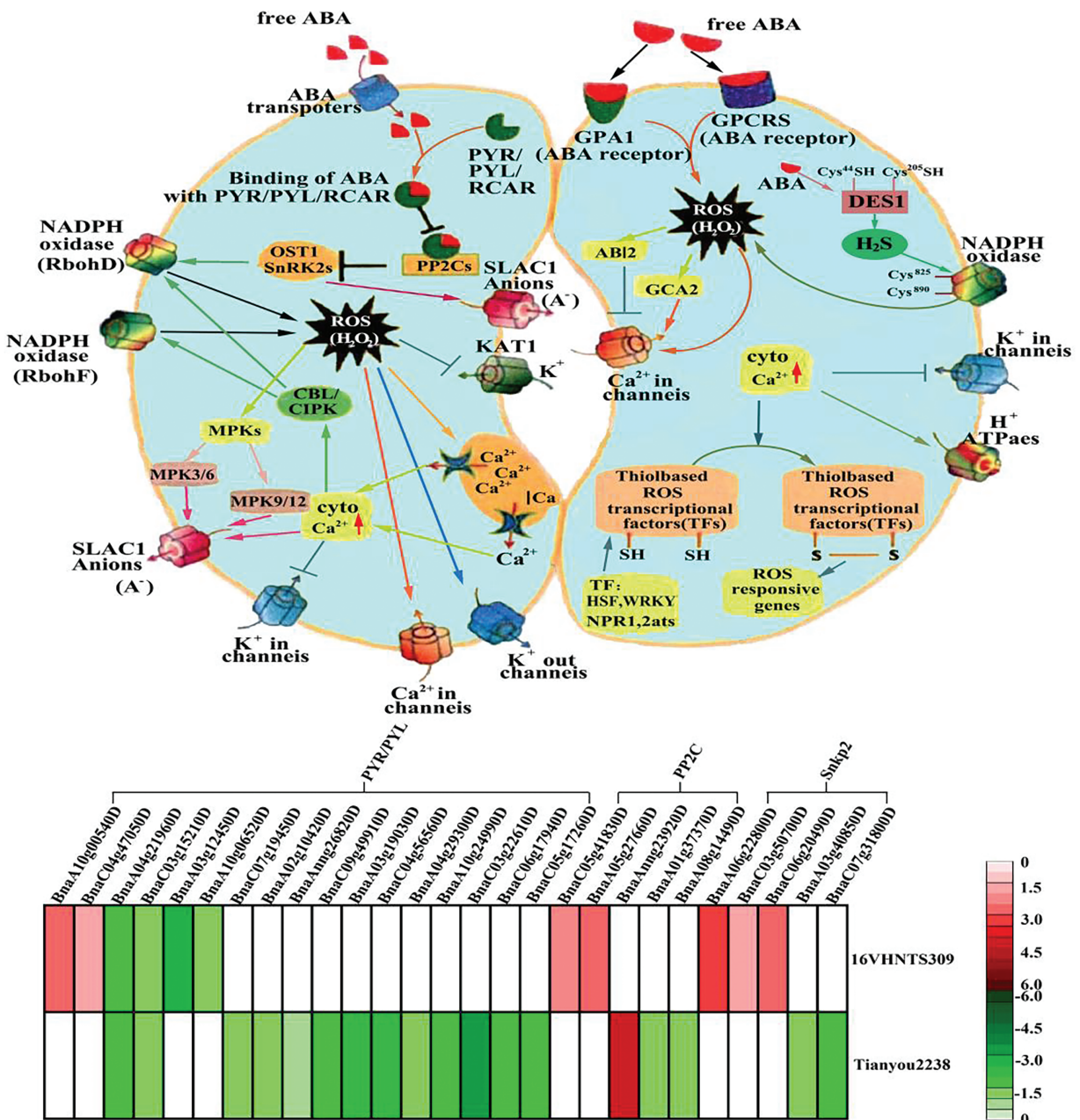


Figure 10: Analysis of the stomatal regulation mechanism of ABA in *B.napus* (quoted from Singh et al. [67])

Acknowledgement: We thank Zibo Yimore Translation Co., Ltd. provided the English text of a draft of this manuscript.

Funding Statement: This study was financially supported by the National Nature Science Foundation Regional Fund Project (32360455); Qingyang City Joint Research Fund Project—Major Project (QY-STK-2024A-046); Doctoral Foundation of Longdong University (XYBYZK2107); University Teachers Innovation Fund Project of Gansu Province (2025A-198).

Author Contributions: Weiliang Qi conceived and designed the study. Weiliang Qi, Cairong Yang, Wancang Sun, Li Ma, Haiqing Liu, and Ziyao Wei conducted the experiments and analyzed the data. Weiliang Qi and Xiaolong Li wrote the manuscript. All authors reviewed the results and approved the final version of the manuscript.

Availability of Data and Materials: Not applicable.

Ethics Approval: Not applicable.

Conflicts of Interest: The authors declare no conflicts of interest to report regarding the present study.

Appendix A

Table A1: The alignment statistics result with the reference gene for all samples

Materials	Raw data					Clean data					Mapping	
	Total reads count (#)	Total bases count (bp)	Q20 bases ratio (%)	Q30 bases ratio (%)	GC bases ratio (%)	Total reads count (#)	Total bases count (bp)	Q20 bases ratio (%)	Q30 bases ratio (%)	GC bases ratio (%)	Total mapped	Uniquely mapped
Tianyou2238_CK_1	57914558	8687183700	97.51	93.54	47.70	55761154	7957582610	98.84	95.90	47.46	92.03	86.14
Tianyou2238_CK_2	66801720	10020258000	97.19	92.88	47.63	63820162	9063467108	98.76	95.69	47.34	91.91	86.15
Tianyou2238_CK_3	57419330	8612899500	97.39	93.44	47.74	55033666	7761687483	98.86	96.01	47.47	91.17	84.96
16VHNTS309_CK_1	90046224	13506933600	98.63	96.16	48.76	88082776	12767565880	99.33	97.51	48.65	92.41	85.83
16HNTS309_CK_2	96669896	14500484400	98.60	96.05	48.74	94410638	13742448149	99.32	97.47	48.65	92.54	85.43
16VHNTS309_CK_3	86295136	12944270400	98.40	95.67	48.17	83825858	12234112384	99.28	97.35	48.09	92.66	86.83
Tianyou2238_cold_1	54104896	8115734400	97.10	92.69	47.89	51507756	7306310622	98.73	95.63	47.61	92.03	86.10
Tianyou2238_cold_2	50621842	7593276300	97.15	92.83	48.29	48128388	6883918893	98.74	95.69	48.05	92.53	86.56
Tianyou2238_cold_3	53326116	7998917400	97.14	92.74	48.03	50799900	7217998490	98.74	95.63	47.78	92.04	86.03
16VHNTS309_cold_1	94066730	14110009500	98.62	96.10	47.97	91939848	13271374069	99.32	97.51	47.85	92.03	85.90
16VHNTS309_cold_2	88582762	13287414300	98.41	95.56	47.90	86258256	12533339805	99.22	97.16	47.79	92.13	85.67
16VHNTS309_cold_3	110701008	16605151200	98.44	95.71	47.57	107753328	15571636943	99.27	97.34	47.43	91.76	85.49

Table A2: DEGs of strong cold hardiness of 16VHNTS309 on GO (Top30) classification

GO.ID	Term	Ontology	Significant	q-Value
GO:0016491	Oxido reductase activity	MF	515/3583	4.57E – 20
GO:0048037	Cofactor binding	MF	351/3583	9.26E – 17
GO:0003824	Catalytic activity	MF	1906/3583	9.87E – 14
GO:1901605	Alpha-amino acid metabolic process	BP	104/2490	8.79E – 12
GO:0055114	Oxidation-reduction process	BP	464/2490	2.33E – 11
GO:0044281	Small molecule metabolic process	BP	357/2490	8.05E – 11
GO:0005506	Iron ion binding	MF	160/3583	2.47E – 10
GO:0044283	Small molecule biosynthetic process	BP	165/2490	1.12E – 09
GO:0019752	Carboxylic acid metabolic process	BP	234/2490	2.01E – 09
GO:0043436	Oxoacid metabolic process	BP	234/2490	2.01E – 09
GO:0006082	Organic acid metabolic process	BP	234/2490	2.14E – 09
GO:0000103	Sulfate assimilation	BP	16/2490	3.02E – 09
GO:0046906	Tetrapyrrole binding	MF	155/3583	1.04E – 08
GO:0005576	Extracellular region	CC	75/1122	1.21E – 08
GO:0020037	Heme binding	MF	152/3583	1.87E – 08
GO:0016829	Lyase activity	MF	99/3583	2.29E – 08
GO:0046394	Carboxylic acid biosynthetic process	BP	142/2490	2.49E – 08
GO:0016053	Organic acid biosynthetic process	BP	142/2490	2.51E – 08
GO:0008652	Cellular amino acid biosynthetic process	BP	81/2490	2.51E – 08
GO:0006790	Sulfur compound metabolic process	BP	63/2490	2.59E – 08
GO:0050662	Coenzyme binding	MF	176/3583	8.48E – 08

(Continued)

Table A2 (continued)

GO.ID	Term	Ontology	Significant	q-Value
GO:1901607	Alpha-amino acid biosynthetic process	BP	69/2490	9.59E – 08
GO:0006576	Cellular biogenic amine metabolic process	BP	31/2490	9.59E – 08
GO:0044106	Cellular amine metabolic process	BP	31/2490	9.59E – 08
GO:0006520	Cellular amino acid metabolic process	BP	143/2490	9.59E – 08
GO:0005975	Carbohydrate metabolic process	BP	266/2490	9.74E – 08
GO:0005509	Calcium ion binding	MF	112/3583	1.23E – 07
GO:0004096	Catalase activity	MF	11/3583	1.36E – 07
GO:0016161	Beta-amylase activity	MF	15/3583	3.59E – 07

Table A3: DEGs of weak cold stress of Tianyou2238 on GO (Top30) classification

GO.ID	Term	Ontology	Significant	q-Value
GO:0005840	Ribosome	CC	544/2002	5.59E – 29
GO:1990904	Ribonucleoprotein complex	CC	556/2002	5.59E – 29
GO:0043228	Non-membrane-bounded organelle	CC	658/2002	5.59E – 29
GO:0043232	Intracellular non-membrane-bounded organelle	CC	658/2002	5.59E – 29
GO:0044444	Cytoplasmic part	CC	709/2002	5.59E – 29
GO:0005737	Cytoplasm	CC	856/2002	5.59E – 29
GO:0032991	Protein-containing complex	CC	789/2002	5.59E – 29
GO:0006412	Translation	BP	609/3654	1.23E – 28
GO:0043043	Peptide biosynthetic process	BP	615/3654	1.23E – 28
GO:0043604	Amide biosynthetic process	BP	628/3654	1.23E – 28
GO:0006518	Peptide metabolic process	BP	626/3654	1.23E – 28
GO:0043603	Cellular amide metabolic process	BP	643/3654	1.23E – 28
GO:1901566	Organonitrogen compound biosynthetic process	BP	841/3654	1.23E – 28
GO:0044271	Cellular nitrogen compound biosynthetic process	BP	740/3654	1.23E – 28
GO:0034645	Cellular macromolecule biosynthetic process	BP	669/3654	1.23E – 28
GO:0009059	Macromolecule biosynthetic process	BP	670/3654	1.23E – 28
GO:0010467	Gene expression	BP	672/3654	1.23E – 28
GO:0044249	Cellular biosynthetic process	BP	987/3654	1.23E – 28
GO:1901576	Organic substance biosynthetic process	BP	997/3654	1.23E – 28
GO:0009058	Biosynthetic process	BP	1055/3654	1.23E – 28
GO:0034641	Cellular nitrogen compound metabolic process	BP	889/3654	1.23E – 28
GO:0003735	Structural constituent of ribosome	MF	543/5111	6.17E – 28
GO:0005198	Structural molecule activity	MF	571/5111	6.17E – 28

(Continued)

Table A3 (continued)

GO.ID	Term	Ontology	Significant	q-Value
GO:0043226	Organelle	CC	983/2002	4.78E – 24
GO:0043229	Intracellular organelle	CC	983/2002	4.78E – 24
GO:0044424	Intracellular part	CC	1234/2002	5.87E – 19
GO:0044391	Ribosomal subunit	CC	75/2002	1.88E – 15
GO:0006520	Cellular amino acid metabolic process	BP	213/3654	4.60E – 13
GO:0015935	Small ribosomal subunit	CC	47/2002	7.82E – 13

Table A4: KEGG (q-Value < 0.05) enriched DEGs in 16VHNTS309, under cold stress

No.	Id	Description	Significant	Annotated	q-Value
1	ko00920	Sulfur metabolism	46/1372	116/14173	0.000
2	ko00196	Photosynthesis-antenna proteins	32/1372	62/14173	0.000
3	ko00966	Glucosinolate biosynthesis	21/1372	30/14173	0.000
4	ko01230	Biosynthesis of amino acids	129/1372	690/14173	0.000
5	ko00380	Tryptophan metabolism	43/1372	139/14173	0.000
6	ko00400	Phenylalanine, tyrosine and tryptophan biosynthesis	39/1372	137/14173	0.000
7	ko04918	Thyroid hormone synthesis	20/1372	59/14173	0.000
8	ko04213	Longevity regulating pathway-multiple species	31/1372	125/14173	0.000
9	ko00630	Glyoxylate and dicarboxylate metabolism	46/1372	226/14173	0.000
10	ko00480	Glutathione metabolism	50/1372	255/14173	0.000
11	ko01200	Carbon metabolism	113/1372	751/14173	0.000
12	ko00906	Carotenoid biosynthesis	22/1372	80/14173	0.000
13	ko01210	2-Oxocarboxylic acid metabolism	40/1372	204/14173	0.000
14	ko00260	Glycine, serine and threonine metabolism	38/1372	193/14173	0.000
15	ko00280	Valine, leucine and isoleucine degradation	27/1372	124/14173	0.001
16	ko04211	Longevity regulating pathway-mammal	33/1372	167/14173	0.001
17	ko00980	Metabolism of xenobiotics by cytochrome P450	29/1372	141/14173	0.001
18	ko00450	Selenocompound metabolism	15/1372	53/14173	0.001
19	ko04212	Longevity regulating pathway-worm	33/1372	173/14173	0.001
20	ko00982	Drug metabolism-cytochrome P450	29/1372	146/14173	0.001
21	ko00270	Cysteine and methionine metabolism	49/1372	298/14173	0.001
22	ko04612	Antigen processing and presentation	15/1372	56/14173	0.002
23	ko00072	Synthesis and degradation of ketone bodies	7/1372	15/14173	0.002
24	ko00130	Ubiquinone and other terpenoid-quinone biosynthesis	24/1372	116/14173	0.002

(Continued)

Table A4 (continued)

No.	Id	Description	Significant	Annotated	q-Value
25	ko00720	Carbon fixation pathways in prokaryotes	19/1372	84/14173	0.002
26	ko00620	Pyruvate metabolism	39/1372	231/14173	0.003
27	ko04922	Glucagon signaling pathway	35/1372	202/14173	0.003
28	ko00261	Monobactam biosynthesis	11/1372	38/14173	0.004
29	ko00360	Phenylalanine metabolism	23/1372	117/14173	0.005
30	ko00860	Porphyrin and chlorophyll metabolism	23/1372	120/14173	0.006
31	ko00330	Arginine and proline metabolism	28/1372	158/14173	0.007
32	ko04626	Plant-pathogen interaction	22/1372	115/14173	0.008
33	ko04621	NOD-like receptor signaling pathway	6/1372	15/14173	0.010
34	ko00401	Novobiocin biosynthesis	7/1372	20/14173	0.010
35	ko00650	Butanoate metabolism	12/1372	49/14173	0.010
36	ko00909	Sesquiterpenoid and triterpenoid biosynthesis	11/1372	43/14173	0.010
37	ko04923	Regulation of lipolysis in adipocyte	9/1372	32/14173	0.013
38	ko00960	Tropane, piperidine and pyridine alkaloid biosynthesis	18/1372	92/14173	0.013
39	ko04915	Estrogen signaling pathway	13/1372	59/14173	0.017
40	ko00950	Isoquinoline alkaloid biosynthesis	12/1372	53/14173	0.018
41	ko04540	Gap junction	12/1372	55/14173	0.024
42	ko00520	Amino sugar and nucleotide sugar metabolism	49/1372	352/14173	0.025
43	ko01212	Fatty acid metabolism	30/1372	194/14173	0.028
44	ko04145	Phagosome	40/1372	278/14173	0.029
45	ko00053	Ascorbate and aldarate metabolism	22/1372	133/14173	0.035
46	ko04723	Retrograde endocannabinoid signaling	9/1372	38/14173	0.035
47	ko00253	Tetracycline biosynthesis	6/1372	20/14173	0.037
48	ko00910	Nitrogen metabolism	19/1372	112/14173	0.040
49	ko04146	Peroxisome	36/1372	252/14173	0.041
50	ko00670	One carbon pool by folate	11/1372	53/14173	0.041
51	ko04068	FoxO signaling pathway	27/1372	177/14173	0.041
52	ko00250	Alanine, aspartate and glutamate metabolism	24/1372	153/14173	0.041
53	ko00660	C5-Branched dibasic acid metabolism	7/1372	27/14173	0.041
54	ko00905	Brassinosteroid biosynthesis	7/1372	27/14173	0.041
55	ko00100	Steroid biosynthesis	16/1372	91/14173	0.043
56	ko00062	Fatty acid elongation	16/1372	92/14173	0.047
57	ko04016	MAPK signaling pathway-plant	45/1372	335/14173	0.047

Table A5: KEGG (q-Value < 0.05) enriched DEGs in tianyou2238, under cold stress

No.	Id	Description	Significant	Annotated	q-Value
1	ko03010	Ribosome	529/2289	1063/14173	0.000
2	ko00400	Phenylalanine, tyrosine and tryptophan biosynthesis	42/2289	137/14173	0.002
3	ko04612	Antigen processing and presentation	22/2289	56/14173	0.002
4	ko01230	Biosynthesis of amino acids	150/2289	690/14173	0.003
5	ko00945	Stilbenoid, diarylheptanoid and gingerol biosynthesis	19/2289	55/14173	0.026
6	ko00360	Phenylalanine metabolism	33/2289	117/14173	0.026
7	ko00062	Fatty acid elongation	27/2289	92/14173	0.035
8	ko02024	Quorum sensing	49/2289	200/14173	0.040
9	ko00966	Glucosinolate biosynthesis	12/2289	30/14173	0.040
10	ko00920	Sulfur metabolism	31/2289	116/14173	0.058

References

- Wang Y, Wang J, Sarwar R, Zhang W, Geng R, Zhu KM, et al. Research progress on the physiological response and molecular mechanism of cold response in plants. *Front Plant Sci.* 2024;15:1334913. doi:10.3389/fpls.2024.1334913.
- Liu LJ, Pu YY, Fang Y, Ma L, Yang G, Niu ZX, et al. Genome-wide analysis of DNA methylation and transcriptional changes associated with overwintering memory in *Brassica rapa* L. grown in the field. *Chem Biol Technol Agric.* 2024;11(1):132. doi:10.1186/s12870-019-1670-9.
- Singh A, Kumar A, Yadav S, Singh I. Reactive oxygen species-mediated signaling during abiotic stress. *Plant Gene.* 2019;18:100173. doi:10.1016/j.plgene.2019.100173.
- Qi W, Wang F, Ma L, Qi Z, Liu S, Chen C, et al. Physiological and biochemical mechanisms and cytology of cold tolerance in *Brassica napus*. *Front Plant Sci.* 2020;11:1241. doi:10.3389/fpls.2020.01241.
- Xu Y, Zhang S, Zhang M, Jiao S, Guo Y, Jiang T. The role of reactive oxygen species in plant-virus interactions. *Plant Cell Rep.* 2024;43(8):197. doi:10.1007/s00299-024-03280-1.
- Yoshioka H, Hino Y, Iwata K, Ogawa T, Yoshioka M, Ishihama N, et al. Dynamics of plant immune MAPK activity and ROS signaling in response to invaders. *Physiol Mol Plant Pathol.* 2023;125:102000. doi:10.1016/j.pmpp.2023.102000.
- Mahiwal S, Pahuja S, Pandey GK. Structural-functional relationship of WRKY transcription factors: unfolding the role of WRKY in plants. *Int J Biol Macromol.* 2024;257(Pt 2):128769. doi:10.1016/j.ijbiomac.2023.128769.
- Choudhary A, Sharma S, Kaur H, Sharma N, Gadewar MM, Mehta S, et al. Plant system, abiotic stress resilience, reactive oxygen species, and coordination of engineered nanomaterials: a review. *S Afr J Bot.* 2024;171(2):45–59. doi:10.1016/j.sajb.2024.05.053.
- Ding C, Hao X, Wang L, Li N, Huang J, Zeng J, et al. iTRAQ-based quantitative proteomic analysis of tea plant (*Camellia sinensis* (L.) O. Kuntze) during cold acclimation and de-acclimation procedures. *Beverage Plant Res.* 2023;3(1):16. doi:10.48130/BPR-2023-0016.
- Desikan RAH, Mackerness S, Hancock JT, Neill SJ. Regulation of the Arabidopsis transcriptome by oxidative stress. *Plant Physiol.* 2001;127(1):159–72. doi:10.1104/pp.127.1.159.
- Wang XC, Zhao QY, Ma CL, Zhang ZH, Cao HL, Kong YM, et al. Global transcriptome profiles of camellia sinensis during cold acclimation. *BMC Genomics.* 2013;14:1–15. doi:10.1186/1471-2164-14-415.
- Wang M, Zhang X, Liu JH. Deep sequencing-based characterization of transcriptome of trifoliolate orange (*Poncirus trifoliata* L. Raf.) in response to cold stress. *BMC Genomics.* 2015;16(1):1–20. doi:10.1186/1471-2164-14-415.
- Liu Y, Jiang Y, Lan J, Zou Y, Gao J. Comparative transcriptomic analysis of the response to cold acclimation in *eucalyptus dunnii*. *PLoS One.* 2014;9(11):e113091. doi:10.1371/journal.pone.0113091.
- Moliterni VMC, Paris R, Onofri C, Orrù L, Cattivelli L, Pacifico D, et al. Early transcriptional changes in beta vulgaris in response to low temperature. *Planta.* 2015;242:187–201. doi:10.1007/s00425-015-2299-z.

15. Wu JY, Pan QW, Fahim AM, Zhang LL, Gong H, Liu LJ, et al. Effects of exogenous calcium and calcium inhibitor on physiological characteristics of winter turnip rape (*Brassica rapa*) under low temperature stress. *BMC Plant Biol.* 2024;24(1):937. doi:10.1186/s12870-024-05556-w.
16. Zhang F. A new spectral index for monitoring leaf area index of winter oilseed rape (*Brassica napus* L.) under different coverage methods and nitrogen treatments. *Plants.* 2024;13(14):1901. doi:10.3390/plants13141901.
17. Chen J, Luo M, Li S, Tao M, Ye X, Duan W, et al. A comparative study of distant hybridization in plants and animals. *Sci China Life Sci.* 2018;61:285–309. doi:10.1007/s11427-017-9094-2.
18. Zhao Y, Mi C, Sun W, Liu Z, Wu J, Fang Y, et al. Analysis of botanical traits and self-compatibility in winter rapeseed *Brassica napus* and *Brassica Rapa* and F1 hybrid populations. *Acta Prataculturae Sinica.* 2016;25(3):108–19. doi:10.11686/cyxb2015103.
19. Wang XF, Tian JH, Zhang YW, Zhang YF, Li DR. New early mature rapeseed germplasms created by *Brassica napus* × *Brassica campestris*. *Chin Agric Sci Bull.* 2017;33(32):28–33.
20. Ma L, Coulter JA, Liu L, Zhao Y, Chang Y, Pu Y, et al. Transcriptome analysis reveals key cold stress responsive genes in winter rapeseed (*Brassica rapa* L.). *Int J Mol Sci.* 2019;20(5):1071. doi:10.3390/ijms20051071.
21. Lai D, Mao Y, Zhou H, Li F, Wu M, Zhang J, et al. Endogenous hydrogen sulfide enhances salt tolerance by coupling the reestablishment of redox homeostasis and preventing salt-induced K⁺ loss in seedlings of *Medicago sativa*. *Plant Sci.* 2014;225:117–29. doi:10.1016/j.plantsci.2014.06.006.
22. Liu X, Wang C, Xu Q, Zhao D, Liu F, Han B. Metabolic response of the lycium barbarum variety ‘Ningqi No. 7’ to drought stress. *Plants.* 2024;13(14):1935. doi:10.3390/plants13141935.
23. Ehrenshaft M, Bilski P, Li MY, Chignell CF, Daub ME. A highly conserved sequence is a novel gene involved in *de novo* vitamin B₆ biosynthesis. *Proc Natl Acad Sci.* 1999;96(16):9374–8. doi:10.1073/pnas.96.16.9374.
24. Mittenhuber G. Phylogenetic analyses and comparative genomics of vitamin B₆ (pyridoxine) and pyridoxal phosphate biosynthesis pathways. *J Mol Microbiol Biotechnol.* 2001;3(1):1–20.
25. Fitzpatrick TB, Moccand C, Roux C. Vitamin B₆ biosynthesis: charting the mechanistic landscape. *ChemBioChem.* 2010;11(9):1185–93.
26. Mooney S, Hellmann H. Vitamin B6: killing two birds with one stone? *Phytochemistry.* 2010;71(5–6):495–501. doi:10.1016/j.phytochem.2009.12.015.
27. Chen H, Xiong L. Pyridoxine is required for post-embryonic root development and tolerance to osmotic and oxidative stresses. *Plant J.* 2005;44(3):396–408. doi:10.1111/j.1365-313X.2005.
28. Benabdellah K, Azcón-Aguilar C, Valderas A, Speziga D, Fitzpatrick TB, Ferrol N. GintPDX1 encodes a protein involved in vitamin B6 biosynthesis that is up-regulated by oxidative stress in the arbuscular mycorrhizal fungus *Glomus intraradices*. *New Phytol.* 2009;184(3):682–93. doi:10.1111/j.1469-8137.2009.02978.x.
29. Raschke M, Boycheva S, Crèvecoeur M, Nunes-Nesi A, Witt S, Fernie AR, et al. Enhanced levels of vitamin B6 increase aerial organ size and positively affect stress tolerance in *Arabidopsis*. *Plant J.* 2011;66(3):414–32. doi:10.1111/j.1365-313X.2011.04499.x.
30. Huang SH, Zhang JY, Wang LH, Huang LQ. Effect of abiotic stress on the abundance of different vitamin B₆ vitamers in tobacco plants. *Plant Physiol Biochem.* 2013;66:63–7. doi:10.1016/j.plaphy.2013.02.010.
31. Falter C, Reumann S. The essential role of fungal peroxisomes in plant infection. *Mol Plant Pathol.* 2022;23(6):781–794. doi:10.1111/mpp.13180.
32. Sandalio LM, Peláez-Vico MA, Molina-Moya E, Romero-Puertas MC. Peroxisomes as redox-signaling nodes in intracellular communication and stress responses. *Plant Physiol.* 2021;186(1):22–35. doi:10.1093/plphys/kiab060.
33. Knoops K, Manivannan S, Capińska MN, Krikken AM, Kram AM, Veenhuis M, et al. Preperoxisomal vesicles can form in the absence of PEX₃. *J Cell Biol.* 2014;204(5):659–68. doi:10.1083/jcb.201310148.
34. Pan D, Nakatsu T, Kato H. Crystal structure of peroxisomal targeting signal-2 bound to its receptor complex Pex7p-Pex21p. *Nat Struct Mol Biol.* 2013;20(8):987–93. doi:10.1038/nsmb.2618.
35. Okumoto K, Noda H, Fujiki Y. Distinct modes of ubiquitination of peroxisome-targeting signal type 1 (PTS1) receptor Pex5p regulate PTS1 protein import. *J Biol Chem.* 2014;289(20):14089–108.

36. Rodrigues TA, Alencastre IS, Francisco T, Brites P, Fransén M, Grou CP, et al. A PEX7-centered perspective on the peroxisomal targeting signal type 2-mediated protein import pathway. *Mol Cell Biol*. 2014;34(15):2917–28. doi:10.1128/MCB.01727-13.
37. Sandalio LM, Collado-Arenal AM, Romero-Puertas MC. Deciphering peroxisomal reactive species interactome and redox signalling networks. *Free Radic Biol Med*. 2023;197(14):58–70. doi:10.1016/j.freeradbiomed.2023.01.014.
38. Mano S, Nakamori C, Nito K, Kondo M, Nishimura M. The *Arabidopsis* pex12 and pex13 mutants are defective in both PTS1- and PTS2-dependent protein transport to peroxisomes. *Plant J*. 2006;47(4):604–18. doi:10.1111/j.1365-313X.2006.02809.x.
39. Pedrosa AG, Francisco T, Bicho D, Dias AF, Barros-Barbosa A, Hagmann V, et al. Peroxisomal monoubiquitinated PEX5 interacts with the AAA ATPases PEX1 and PEX6 and is unfolded during its dislocation into the cytosol. *J Biol Chem*. 2018;293(29):11553–63. doi:10.1074/jbc.RA118.003669.
40. Gonzalez Kim L, Ratzel SE, Burks KH, Danan CH, Wages JM, Zolman BK, et al. A pex1 missense mutation improves peroxisome function in a subset of *Arabidopsis* pex6 mutants without restoring pex5 recycling. *Proc Natl Acad Sci*. 2018;115(14):E3163–72. doi:10.1073/pnas.1721279115.
41. Ren H, Li Y, Zhao F, Pu X, Wei L, Lv X, et al. The role of autophagy in alleviating damage of aluminum stress in *Arabidopsis thaliana*. *Plant Growth Regul*. 2016;79:167–75. doi:10.1007/s10725-015-0122-2.
42. Shibata M, Oikawa K, Yoshimoto K, Kondo M, Mano S, Yamada K, et al. Highly oxidized peroxisomes are selectively degraded via autophagy in *Arabidopsis*. *Plant Cell*. 2013;25(12):4967–83. doi:10.1105/tpc.113.116947.
43. Yu H, Song L, Han J, Yu X, Wu Y, Yu Z. Exogenous hydrogen sulphide alleviates senescence of postharvest pakchoi through regulating antioxidant system, endogenous hydrogen sulphide and nitric oxide metabolism. *Postharvest Biol Technol*. 2024;207:112632. doi:10.1016/j.postharvbio.2023.112632.
44. Hao X, Cao H, Wang Z, Jia X, Jin ZP, Pei Y. Hydrogen sulfide improves plant drought tolerance by regulating the homeostasis of reactive oxygen species. *Plant Growth Regul*. 2024;9(2):1–9. doi:10.1007/s10725-024-01197-z.
45. Cheng J, Zhang Z, Gao Y, Dong Y, Xian X, Li C, et al. Overexpressing ATP sulfurylase improves Fe-deficiency tolerance in apple calli and tobacco. *Agronomy*. 2024;14(3):404. doi:10.3390/agronomy14030404.
46. Manne H, Kumari N, Yashveer S, Nain S, Duhan J, Avtar R, et al. Mitigation of lead toxicity in *Brassica juncea* L. by sulphur application-Via various biochemical and transcriptomic strategies. *J King Saud Univ-Sci*. 2024;36(5):103175. doi:10.1016/j.jksus.2024.103175.
47. Rotte C, Leustek T. Differential subcellular localization and expression of ATP sulfurylase and 5'-adenylylsulfate reductase during ontogenesis of *Arabidopsis* leaves indicates that cytosolic and plastid forms of ATP sulfurylase may have specialized functions. *Plant Physiol*. 2000;124(2):715–24. doi:10.1104/pp.124.2.715.
48. Lee S, Leustek T. APS kinase from *Arabidopsis thaliana*: genomic organization, expression, and kinetic analysis of the recombinant enzyme. *Biochem Biophys Res Commun*. 1998;247(1):171–5. doi:10.1006/bbrc.1998.8751.
49. Kolupaev YE, Yemets AI, Yastreb TO, Blume YB. The role of nitric oxide and hydrogen sulfide in regulation of redox homeostasis at extreme temperatures in plants. *Front Plant Sci*. 2023;14:1128439. doi:10.3389/fpls.2023.1128439.
50. Swindell J, Dos Santos PC. Interactions with sulfur acceptors modulate the reactivity of cysteine desulfurases and define their physiological functions. *BBA-Mol Cell Res*. 2024;1871(7):119794. doi:10.1016/j.bbamcr.2024.119794.
51. Bhadwal SS, Verma S, Hassan S, Kaur S. Unraveling the potential of hydrogen sulfide as a signaling molecule for plant development and environmental stress responses: a state-of-the-art review. *Plant Physiol Biochem*. 2024;212:108730. doi:10.1016/j.plaphy.2024.108730.
52. Capaldi FR, Gratão PL, Reis AR, Lima LW, Azevedo RA. Sulfur metabolism and stress defense responses in plants. *Trop Plant Biol*. 2015;8(3-4):60–73. doi:10.1007/s12042-015-9152-1.
53. Zheng L, Yu P, Zhang Y, Wang P, Yan W, Guo B, et al. Evaluating the bio-application of biomacromolecule of lignin-carbohydrate complexes (LCC) from wheat straw in bone metabolism via ROS scavenging. *Int J Biol Macromol*. 2021;176(3):13–25. doi:10.1016/j.ijbiomac.2021.01.103.
54. Zheng S, Li J, Ma L, Zhuang C. OsAGO2 controls ROS production and the initiation of tapetal PCD by epigenetically regulating OsHXX1 expression in rice anthers. *Proc Natl Acad Sci*. 2019;116(15):7549–58. doi:10.1073/pnas.1817675116.

55. Lin S, Li Y, Zhao J, Guo W, Jiang M, Li X, et al. Transcriptome analysis of biochemistry responses to low-temperature stress in the flower organs of five pear varieties. *Forests*. 2023;14(3):490–14030490. doi:10.3390/f14030490.
56. Zhang X, Zhang D, Zhong C, Li W, Dinesh-Kumar SP, Zhang Y. Orchestrating ROS regulation: coordinated post-translational modification switches in NADPH oxidases. *New Phytol*. 2025;245(2):510–22. doi:10.1111/nph.20231.
57. Wang H, Feng M, Zhong X, Yu Q, Que Y, Xu L, et al. Identification of Saccharum CaM gene family and function characterization of ScCaM1 during cold and oxidant exposure in *Pichia pastoris*. *Genes Genomics*. 2023;45(1):103–22. doi:10.1007/s13258-022-01263-8.
58. Wang H, Cheng X, Yin D, Chen D, Luo C, Liu H, et al. Advances in the research on plant WRKY transcription factors responsive to external stresses. *Curr Issues Mol Biol*. 2023;45(4):187. doi:10.3390/cimb45040187.
59. Anthony RG, Henriques R, Helfer A, Mészáros T, Rios G, Testerink C, et al. A protein kinase target of a PDK1 signalling pathway is involved in root hair growth in *Arabidopsis*. *EMBO J*. 2004;23(3):572–81.
60. Son Y, Cheong YK, Kim NH, Chung HT, Kang DG, Pae HO. Mitogen-activated protein kinases and reactive oxygen species: how can ROS activate MAPK pathways? *J Signal Transduct*. 2011;2011(1–4):792639–6. doi:10.1155/2011/792639.
61. Singh VP, Jaiswal S, Wang Y, Feng S, Tripathi DK, Singh S, et al. Evolution of reactive oxygen species cellular targets for plant development. *Trends Plant Sci*. 2024;29(8):865–77.
62. Liu J, Wang X, Wu H, Zhu Y, Ahmad I, Dong G, et al. Association between reactive oxygen species, transcription factors, and candidate genes in drought-resistant sorghum. *Int J Mol Sci*. 2024;25(12):6464. doi:10.3390/ijms25126464.
63. Goyal P, Devi R, Verma B, Hussain S, Arora P, Tabassum R, et al. WRKY transcription factors: evolution, regulation, and functional diversity in plants. *Protoplasma*. 2023;260(2):331–48. doi:10.1007/s00709-022-01794-7.
64. Fu QT, Yu DQ. Expression profiles of AtWRKY25, AtWRKY26 and AtWRKY33 under abiotic stresses. *Yi Chuan Hereditas*. 2010;32(8):848–56. doi:10.3724/sp.j.1005.2010.00848.
65. Zhou LX, Cao HX. Expression characteristics of WRKY transcription factor genes in oil palm under low temperature. *J South Agric*. 2018;49(8):1490–7.
66. Zhang J, Wang X, Vikash V, Ye Q, Wu D, Liu Y, et al. ROS and ROS-mediated cellular signaling. *Oxid Med Cell Longev*. 2016;2016(1):4350965. doi:10.1155/2016/4350965.
67. Singh R, Parihar P, Singh S, Mishra RK, Singh VP, Prasad SM. Reactive oxygen species signaling and stomatal movement: current updates and future perspectives. *Redox Biol*. 2017;11:213–8. doi:10.1016/j.redox.2016.11.006.
68. Magrì A, Cubisino SA, Battiato G, Lipari CL, Conti Nibali S, Saab MW, et al. VDACL1 knockout affects mitochondrial oxygen consumption triggering a rearrangement of ETC by impacting on complex I activity. *Int J Mol Sci*. 2023;24(4):3687. doi:10.3390/ijms24043687.
69. Lee SM, Hoang MHT, Han HJ, Kim HS, Lee K, Kim KE, et al. Pathogen inducible voltage-dependent anion channel (AtVDAC) isoforms are localized to mitochondria membrane in *Arabidopsis*. *Mol Cells*. 2009;27:321–7. doi:10.1007/s10059-009-0041-z.
70. Tan W, Colombini M. VDAC closure increases calcium ion flux. *BBA-Biomembr*. 2007;1768(10):2510–5. doi:10.1016/j.bbamem.2007.06.002.
71. Lai JC, Tan W, Benimetskaya L, Stein CA. A pharmacologic target of G3139 in melanoma cells may be the mitochondrial VDAC. *Proc Nat Acad Sci*. 2006;103(19):7494–9. doi:10.1073/pnas.0602217103.
72. Li Y, Chen L, Mu J, Zuo J. LESION SIMULATING DISEASE1 interacts with catalases to regulate hypersensitive cell death in *Arabidopsis*. *Plant Physiol*. 2013;163(2):1059–70. doi:10.1104/pp.113.225805.